

Stability of Circumferential Flaws in Once-Through Steam Generator Tubes Under Thermal Loading During LOCA, MSLB and FWLB

AVAILABILITY OF REFERENCE MATERIALS IN NRC PUBLICATIONS

NRC Reference Material

As of November 1999, you may electronically access NUREG-series publications and other NRC records at the NRC's Public Electronic Reading Room at <http://www.nrc.gov/reading-rm.html>. Publicly released records include, to name a few, NUREG-series publications; *Federal Register* notices; applicant, licensee, and vendor documents and correspondence; NRC correspondence and internal memoranda; bulletins and information notices; inspection and investigative reports; licensee event reports; and Commission papers and their attachments.

NRC publications in the NUREG series, NRC regulations, and Title 10, "Energy," in the *Code of Federal Regulations* may also be purchased from one of these two sources.

1. The Superintendent of Documents

U.S. Government Publishing Office
Mail Stop SSOP
Washington, DC 20402-0001
Internet: <http://bookstore.gpo.gov>
Telephone: 1-866-512-1800
Fax: (202) 512-2104

2. The National Technical Information Service

5301 Shawnee Road
Alexandria, VA 22161-0002
<http://www.ntis.gov>
1-800-553-6847 or, locally, (703) 605-6000

A single copy of each NRC draft report for comment is available free, to the extent of supply, upon written request as follows:

U.S. Nuclear Regulatory Commission

Office of Administration
Publications Branch
Washington, DC 20555-0001
E-mail: distribution.resource@nrc.gov
Facsimile: (301) 415-2289

Some publications in the NUREG series that are posted at the NRC's Web site address <http://www.nrc.gov/reading-rm/doc-collections/nuregs> are updated periodically and may differ from the last printed version. Although references to material found on a Web site bear the date the material was accessed, the material available on the date cited may subsequently be removed from the site.

Non-NRC Reference Material

Documents available from public and special technical libraries include all open literature items, such as books, journal articles, transactions, *Federal Register* notices, Federal and State legislation, and congressional reports. Such documents as theses, dissertations, foreign reports and translations, and non-NRC conference proceedings may be purchased from their sponsoring organization.

Copies of industry codes and standards used in a substantive manner in the NRC regulatory process are maintained at—

The NRC Technical Library

Two White Flint North
11545 Rockville Pike
Rockville, MD 20852-2738

These standards are available in the library for reference use by the public. Codes and standards are usually copyrighted and may be purchased from the originating organization or, if they are American National Standards, from—

American National Standards Institute

11 West 42nd Street
New York, NY 10036-8002
<http://www.ansi.org>
(212) 642-4900

Legally binding regulatory requirements are stated only in laws; NRC regulations; licenses, including technical specifications; or orders, not in NUREG-series publications. The views expressed in contractor-prepared publications in this series are not necessarily those of the NRC.

The NUREG series comprises (1) technical and administrative reports and books prepared by the staff (NUREG-XXXX) or agency contractors (NUREG/CR-XXXX), (2) proceedings of conferences (NUREG/CP-XXXX), (3) reports resulting from international agreements (NUREG/IA-XXXX), (4) brochures (NUREG/BR-XXXX), and (5) compilations of legal decisions and orders of the Commission and Atomic and Safety Licensing Boards and of Directors' decisions under Section 2.206 of NRC's regulations (NUREG-0750).

DISCLAIMER: This report was prepared as an account of work sponsored by an agency of the U.S. Government. Neither the U.S. Government nor any agency thereof, nor any employee, makes any warranty, expressed or implied, or assumes any legal liability or responsibility for any third party's use, or the results of such use, of any information, apparatus, product, or process disclosed in this publication, or represents that its use by such third party would not infringe privately owned rights.

Stability of Circumferential Flaws in Once-Through Steam Generator Tubes Under Thermal Loading During LOCA, MSLB and FWLB

Manuscript Completed: December 2010
Date Published: November 2017

Prepared by:
Saurin Majumdar

Argonne National Laboratory
Argonne, IL 60439

Matt Rossi, NRC Project Manager

NRC Job Code Y6582

ABSTRACT

Axial thermal loads during loss of coolant, main steam line break and feed water line break accident conditions may cause circumferential flaws in steam generator tubes to sever in once-through steam generators (OTSGs). Finite element models were used to examine the combined effects of thermal loads, tube size, flaw size, and accident conditions that result in tube failure.

FOREWORD

This report documents studies conducted by Dr. Saurin Majumdar at Argonne National Laboratory (ANL) and supports the development of a technical basis in evaluating licensee safety analyses of accident scenarios in pressurized water reactors (PWRs) utilizing OTSG designs. Verification of industry safety analyses is important for the evaluation of plant inspections and licensing of steam generators.

Axial thermal loads during loss of coolant accident (LOCA), main steam line break (MSLB), or feedwater line break (FWLB) accident conditions may cause failure of circumferential flaws in OTSG tubes. Finite element models (FEM) were used to examine the combined effects of thermal loads, flaw size, and accident conditions that result in tube failure(s).

For LOCA accidents, a variety of flaws of differing lengths and depths will not compromise tube integrity.

Under MSLB conditions, a literature review of industry analyses showed that there is considerable variance in the reported OTSG tube axial loads between plants. For the purpose of the present report, ANL used a best-estimate axial load value of 2.9 kN (650 lbf) and a bounding axial load value of 13.3 kN (3000 lbf) in the FEM simulations.

For FWLB conditions, a literature review of existing industry analyses showed that stresses due to OTSG tube axial loads during FWLBs are either small or compressive and pose no challenge to the integrity of OTSG tubes with circumferentially oriented flaws.

The results from this study are broadly in agreement with those that have been reported by industry.

TABLE OF CONTENTS

ABSTRACT	iii
FOREWORD.....	v
TABLE OF CONTENTS	vii
LIST OF FIGURES	ix
EXECUTIVE SUMMARY	xi
ACKNOWLEDGMENTS	xiii
ACRONYMS AND ABBREVIATIONS	xv
1 INTRODUCTION	1
1.1 Background.....	1
1.2 ASME Code Perspective	1
1.3 Results from Industry Calculations	2
1.3.1 LBLOCA.....	2
1.3.2 MSLB and FWLB	3
2 ANALYSIS OF OTSG TUBE WITH CIRCUMFERENTIAL DEGRADATION	5
2.1 Assumptions	7
2.2 Loading and Boundary Conditions.....	7
2.3 Material Properties.....	7
2.3.1 Validation of Finite Element Approach.....	8
2.4 Failure Criteria	8
2.4.1 Circumferential Cracks.....	8
2.4.2 Wear Marks.....	12
3 RESULTS FOR LOCA ANALYSES.....	13
3.1 Single Circumferential Cracks.....	13
3.1.1 Single 100 Percent Throughwall Circumferential Crack.....	13
3.1.2 Part-Throughwall 360° Crack.....	15
3.1.3 Single Part-Throughwall Cracks (<360°).....	17
3.1.4 Failure Diagram for Single Circumferential Cracks	22
3.2 Wear Marks at Trefoil TSPs.....	23
3.2.1 Part-Throughwall OD Wear Marks.....	24
3.2.2 100 Percent Throughwall Wear-Induced Cracks	26
3.2.3 Summary of Results for Wear Marks	28
4 RESULTS FOR MSLB	29
4.1 Single 100 Percent Throughwall Circumferential Flaw	29
4.2 Single Part-Throughwall Circumferential Flaw.....	29
5 DISCUSSIONS AND CONCLUSIONS	33
5.1 LOCA.....	33
5.2 MSLB and FWLB	34
6 REFERENCES	35

LIST OF FIGURES

Figure 2-1	Longitudinal cross-section of an OTSG.....	6
Figure 2-2	Engineering and true stress-strain curves of (a) Alloy 600 Heat EX-82-1 and (b) Alloy 600 Heat NX 8520L.....	8
Figure 2-3	Engineering stress-strain curves as measured in uniaxial tensile tests and as predicted by FEA of tensile specimens for Alloy 600 Heats (a) EX-82-1 and (b) NX 8520L	9
Figure 2-4	Typical crack opening geometry and definition of COD for a 100 percent TW crack	10
Figure 2-5	Typical crack opening geometry and definition of COD for a PTW crack.....	10
Figure 2-6	Typical necking initiation in a specimen with 100 percent TW crack.....	11
Figure 3-1	Variation of COD with ΔT for 100 percent TW cracks of various lengths	13
Figure 3-2	Variation of COD with total axial load for 100 percent TW cracks of various lengths	14
Figure 3-3	Variation of peak crack tip equivalent plastic strain through the wall thickness at the critical temperature differences ΔT s for the various cracks obtained from Fig. 3-1	14
Figure 3-4	Variation of critical temperature difference ΔT with 100 percent TW circumferential crack length.....	15
Figure 3-5	Variation of COD of 360° PTW cracks of various depths with temperature difference ΔT	16
Figure 3-6	Variation of peak equivalent plastic strain at the crack tip of 360° PTW cracks of various depths with temperature difference ΔT	16
Figure 3-7	Variations of critical temperature difference with crack depth of 360° circumferential PTW cracks predicted by various failure criteria	17
Figure 3-8	Variation of COD of 90 percent deep PTW cracks of various lengths with temperature difference ΔT	18
Figure 3-9	Variation of peak equivalent plastic strain at the crack tip along the crack front of 90 percent deep (a) 300°, (b) 120°, (c) 60° and (d) 90° cracks.....	19
Figure 3-10	Variation of COD of 80 percent deep PTW cracks of various lengths with temperature difference ΔT	20
Figure 3-11	Variation of peak equivalent plastic strain at the crack tip along the crack front of 80 percent deep (a) 50°, (b) 90°, (c) 120° and (d) 180° cracks.....	20
Figure 3-12	Variation of COD of 60 percent deep 120°, 180°, and 240° PTW cracks of various lengths with temperature difference ΔT	21
Figure 3-13	Variation of peak equivalent plastic strain at the crack tip along the crack front of 60 percent deep (a) 240°, (b) 180°, and (c) 120° cracks.....	22
Figure 3-14	Variations of failure temperatures of 60, 80, 90 percent PTW and 100 percent TW circumferential cracks with crack angle	23

Figure 3-15	Failure map of a circumferential crack in a 15.9 mm (5/8 in.) diameter SG tube subjected to LBLOCA cooldown loading	24
Figure 3-16	Variation of the COD of (a) 60 and (b) 90 percent deep 3x30° and 3x45° PTW wear marks with temperature difference ΔT	25
Figure 3-17	Variation of the equivalent plastic strain along the crack tip of the 90 percent deep (a) 3x30° and (b) 3x45° wear marks with angular distance at various values of ΔT	26
Figure 3-18	Variation of the loads carried by the crack tip PTW ligament, the solid full thickness ligament and the total load with ΔT for (a) 3x30°x90 percent and (b) 3x45°x90 percent PTW cracks.....	26
Figure 3-19	Variation of the COD with (a) temperature difference ΔT and (b) load for 100 percent TW 3x45 cracks. Also shown are lines representing the critical COD for the initiation of unstable tearing.	27
Figure 3-20	Variation of the average equivalent plastic strain in four elements at the crack tip of 100 percent TW 3x45° cracks with ΔT	28
Figure 4-1	Variation of COD with axial load for various 100 percent TW cracks	29
Figure 4-2	Variation of (a) COD and (b) average crack tip plastic strain with axial load for various 90 percent deep PTW cracks.....	30
Figure 4-3	Variation of (a) COD and (b) average crack tip plastic strain with axial load for various 80 percent deep PTW cracks.....	30
Figure 4-4	Critical axial loads for various circumferential crack lengths	31

EXECUTIVE SUMMARY

There is a concern that circumferentially oriented flaws, e.g., cracks at the bottom of the top tubesheet or wear scars under the lands of the tube support plates (TSPs) in SG tubes of once-through steam generators (OTSGs) may be challenged by the thermally induced tensile axial loads during a loss of coolant (LOCA), main steam line break (MSLB) or feed water line break (FWLB) accidents, and cause the tubes to sever.

Elastic-plastic finite element analyses were carried out for a single OTSG tube containing circumferential flaws at the top of the bottom tubesheet subjected to a cooldown loading, simulating the quenching phase of the LOCA transient. Detailed thermal hydraulic analysis of the LOCA event conducted by the industry has shown that the largest temperature difference between the cooled tube and the hot SG shell during the quench phase is 195°C-205°C (350°F-370°F). The current analysis assumed that the SG tube is fixed at both ends and subjected to a linearly ramped cooldown. The lateral supports from the intervening TSPs were included in the model. Circumferential cracks of various morphologies were considered, including single 100 percent throughwall (TW) and part-throughwall (PTW) outer diameter (OD) cracks of various lengths and three PTW OD wear scars of several lengths and depths located 120° apart, symmetrically around the circumference of the tube.

The results are broadly in agreement with those that have been reported by the industry and show that for LOCAs:

- (1) Single 100 percent TW circumferential cracks $\leq 110^\circ$ long will survive (i.e., will not burst unstably) the cooldown without tensile rupture or unstable crack tip tearing;
- (2) Single PTW cracks ≤ 60 percent deep, $\leq 135^\circ$ long will not experience either ligament rupture or unstable crack tip tearing (burst) during the cooldown (i.e., will not leak);
- (3) Single PTW cracks > 60 percent deep, $> 135^\circ$ long will experience unstable crack tip tearing (burst) during the cooldown (i.e., will have large leak rate);
- (4) Single PTW cracks > 60 percent deep, $\leq 110^\circ$ long may, depending on their length/depth, either experience ligament rupture (i.e., will leak) without unstable tearing (burst) or survive the cooldown without ligament rupture or unstable tearing (burst) (i.e., will not leak);
- (5) Single 360° PTW cracks > 31 percent deep will fail by tensile rupture during the cooldown (i.e., will have large leak rate);
- (6) 60 percent deep, 3x30° and 3x45° long PTW wear marks will survive the cooldown without ligament rupture (i.e., will not leak);
- (7) 3x90 percent deep wear marks each $\leq 27.5^\circ$ long will survive the cooldown without ligament rupture (i.e., will not leak).
- (8) 90 percent deep 3x30° and 3x45° OD wear marks will suffer ligament rupture (i.e., will leak) during the cooldown but will not experience unstable burst.

For MSLB conditions, a literature review of existing industry analyses showed that there is considerable variability in the reported OTSG tube axial loads between plants. For the purpose

of the present report, we used a best-estimate axial load value of 2891 N (650 lbf) and a bounding axial load value of 13344 N (3000 lbf). Our analyses indicate that for MSLBs:

- (1) Single circumferential cracks $\leq 330^\circ$ long, ≤ 90 percent deep, will survive the best-estimate axial load without ligament rupture or unstable tearing;
- (2) Single 100 percent TW cracks $< 170^\circ$ long will survive the bounding value of the axial load without unstable tearing;
- (3) Single 90 percent deep PTW cracks $< 100^\circ$ and single 80 percent deep PTW cracks $< 140^\circ$ will survive the bounding value of the axial load without ligament rupture or unstable tearing;
- (4) Single 80 percent deep cracks $> 140^\circ$ but $< 170^\circ$ will undergo ligament rupture but not unstable tearing due to the bounding value of the axial load;
- (5) Single 90 percent deep cracks $> 100^\circ$ but $< 170^\circ$ will undergo ligament rupture but not unstable tearing due to the bounding value of the axial load.

For FWLB conditions, a literature review of existing industry analyses showed that there is a consensus that stresses due to OTSG tube axial loads during FWLBs are either small or compressive and pose no challenge to circumferentially oriented flaws.

ACKNOWLEDGMENTS

The author wishes to thank Kenneth Karwoski for his support. This work was sponsored by the Office of Nuclear Regulatory Research, U. S. Nuclear Regulatory Commission; Program Manager: Matt Rossi.

ACRONYMS AND ABBREVIATIONS

ASME	American Society of Mechanical Engineers
B&W	Babcock and Wilcox
B&WOG	Babcock and Wilcox Owners Group
COD	Crack opening displacement
CODSCC	Circumferential outer diameter stress corrosion crack
RG	Regulatory Guide
EOTSG	Enhanced Once Through Steam Generator
EPRI	Electric Power Research Institute
FEA	Finite element analysis
FWLB	Feed water line break
ID	Inner diameter
LBB	Leak before break
LBLOCA	Large break LOCA
LOCA	Loss of coolant accident
LPI	Low pressure injection
MA	Mill annealed
MSLB	Main steam line break
NRC	Nuclear Regulatory Commission
OD	Outer diameter
ODSCC	Outer diameter stress corrosion crack
OTSG	Once-through steam generator
PTW	Part-throughwall
RCS	Reactor coolant system
SG	Steam generator
SGTR	Steam generator tube rupture
TSP	Tube support plate
TW	Throughwall

1 INTRODUCTION

There is a concern that circumferentially oriented flaws, e.g., cracks at the bottom of the top tubesheet or wear scars under the lands of the TSPs in OTSG tubes may be challenged by the thermally induced tensile axial loads during LOCAs, MSLB and FWLB accidents and cause the tubes to sever.

The objective of the present study was to determine the longest circumferential flaws that a typical SG tube in an OTSG can tolerate without undergoing ligament rupture and/or unstable burst during the cooldown period of a LOCA, MSLB or FWLB accident. Elastic-plastic finite-element analyses (FEAs) were conducted on a typical OTSG tube fixed at both ends and subjected to a cooldown loading. For simplicity, the models analyzed included a full-length tube containing a single outer-diameter (OD) part-throughwall (PTW) circumferential crack of various lengths and depths as well as three OD circumferential wear scars of several lengths and depths located symmetrically around the circumference of the tube.

1.1 Background

Industry analyses of large-bore RCS pipe breaks and subsequent large break loss of coolant accidents (LBLOCAs) show that the integrity of OTSG tubes with circumferential cracks may be challenged due to axial tensile loads imposed during the quenching phase of the accident (Refs. 1, 2). Similar concerns also exist for OTSG tubes subjected to MSLB and FWLB accidents. Flaws have been historically analyzed by industry for satisfying acceptance criteria for integrity and leakage assessment after each inspection (Refs. 3-5).

The LOCA of concern is a break in the upper hot leg large-bore piping. Low pressure injection (LPI) refills the RCS including the hot leg and OTSG tube regions of the broken loop and a continuous liquid flow through the OTSG tubes and out the break is established. This liquid throughput can eventually result in a large SG tube-to-shell temperature difference, which can induce high axial loads and result in a steam generator tube rupture (SGTR) if there is a "large" flaw in the tube. These loads result from the differential thermal expansion between the OTSG tubes and the shell, which is rigidly attached to the tubesheets at both ends.

1.2 ASME Code Perspective

The Boiler and Pressure Vessels Code of the American Society of Mechanical Engineers (ASME Code) currently allows exclusion of secondary stresses (i.e., thermal stresses) from the OTSG for faulted conditions. In fact, the ASME Code allows exclusion of all but the primary OTSG loads. Per the ASME Code criteria, the pressure load from a LBLOCA is a primary load for the steam generators. However, this pressure load is small relative to other design basis events, such as MSLB and FSLB. For most of the OTSG parts (e.g., shell, heads, tubesheets), the thermal loads are classified as secondary stress per the ASME Code criteria and hence do not require evaluation. However, for degraded steam generator tubes, the axial thermal load associated with the postulated large-bore RCS pipe break event may not satisfy the ASME secondary stress classification. This is due to the large strains associated with the tube load and the potential for the strain to concentrate at a flaw in the tube (localized yielding). Therefore, these thermal loads have to be treated as primary loading. Note that tube failure due to strain concentrations is not a concern in un-degraded tubes since the strains are evenly distributed over the entire length of the tube.

Regulatory Guide 1.121, *Bases for Plugging Degraded PWR Steam Generator Tubes*, (RG 1.121) contains the guidance for determining how plugging limits are determined, including required safety margins. In general, RG 1.121 enforces the design requirements of the ASME Code, and in addition specifies that tubes shall have a margin to burst of 3.0 for normal operating conditions, and 1.4 for faulted conditions. All PWRs in the US also have requirements in their technical specifications regarding the required safety margins needed for demonstrating tube integrity.

1.3 Results from Industry Calculations

1.3.1 LBLOCA

BAW-2374 (Ref. 2) reported that when a postulated LBLOCA is included, the maximum plant-specific shell-to-tube thermal difference would be increased to between 195°C and 205°C (350°F and 370°F). The maximum tube axial load resulting from the LBLOCA event was estimated to be approximately 17.1 kN (3850 lbf). This load is also similar to the limiting upper tolerance yield load of the OTSG tubing, 17.3 kN (3900 lbf). The LBLOCA transient results in a reduction of pressure in both the primary and secondary side of the steam generators. When the primary side begins to refill with cold water and cools the tubes creating the large axial loads, the pressure difference between the primary and secondary sides (ΔP) is expected to be less than 0.7 MPa (100 psi). At the time of maximum tube load and dilation (volume expansion), the ΔP is estimated to be approximately 0.7 MPa (45 psi). Therefore, there are no significant stresses or dilations (volume expansions) resulting from the pressure loads associated with the LBLOCA event.

An evaluation was performed to determine the allowable circumferential extent for a 60 percent through-wall (TW) flaw for the limiting axial tube loads associated with tube yield strengths (lower tolerance yield load of 12.9 kN [2900 lbf], average yield load of 15.1 kN [3400 lbf], and upper tolerance yield load of 17.3 kN [3900 lbf]). The evaluation determined the circumferential extent at which net section collapse is expected to occur. It is noted that the upper tolerance yield load of 17.3 kN (3900 lbf) is slightly greater than the estimated maximum load of 17.1 kN (3850 lbf) for the large-bore RCS pipe break. The flow stress associated with the yield stress used in the limiting load calculation is also used in determining the critical flaw size for that load. The results of the analysis showed that for the limiting upper tolerance yield load of 17.3 kN (3900 lbf), the allowable extent of a 60 percent TW flaw was 80 degrees for a free-span flaw and 150 degrees for a flaw constrained by the tubesheet.

For an assumed ΔP of 0.7 MPa (45 psi) and a fluid temperature of 20°C (70°F), the calculated leakage ranged from 8×10^{-4} L/min (2×10^{-4} gpm) for a 1.3 mm (0.05 in.) long flaw to 5.6 L/min (1.5 gpm) for a 23 mm (0.90 in.) long (circumferential extent of 165 degrees) flaw.

Two types of service-induced degradation (wear) have been found in the Oconee replacement OTSGs (Ref. 6). These include wear at the land contacts in the broached tube support plate openings and wear at drilled support plate openings (drilled support plate openings only occur in the periphery region at the 14th support plate). The best estimate structural integrity limit for wear at the land contact area is 78 percent TW and for wear at the drilled hole opening is 54 percent TW with a circumferential extent of 25 mm (0.98 in.) (180 degrees).

In a submittal to NRC in 2010 in regard to Davis Besse nuclear power station (Ref. 7), the licensee has cited new experimental results for axial strengths of OTSG tubes with circumferential EDM slots of various lengths and depths. They have recalculated the maximum

50/50 structural limit for a 100 percent TW circumferential flaw under yield point loading to be 14 mm (0.55 in.) (107 degrees). Axial pull tests have also shown that wear scar maximum depth must be >92 percent for it to pop through at yield point axial load. Wear scars detected during the 2008 outage inspection could reach 100 percent TW and still meet the LBLOCA structural integrity criterion at 95/50 (Ref. 7).

In January 2010, AREVA performed a thermal hydraulic evaluation of thermal loads on the TMI-1 replacement steam generator at 100 percent power and hot zero power. AREVA used the results of these analyses, which are summarized in an AREVA Report (Ref. 8), to conclude that:

The only portions of the EOTSG significantly affected by the LBLOCA loads are the tube-to-tubesheet weld and tubes with potential wear degradation.

The allowable pop-through depth for a TSP wear scar is 78 percent TW. The ligament pop-through will not lead to a tube "burst".

The Technical Specification 40 percent TW plugging limit (end-of-cycle) was demonstrated to be conservative and appropriate for circumferential degradation associated with wear type defects detected during inspection.

1.3.2 MSLB and FWLB

Reference 3 is the earliest report on the subject. It establishes the analytical and experimental justifications for establishing the minimum steam generator tube wall thickness for B&W 177-FA nuclear steam systems in accordance with NRC Regulatory Guide 1.121. First, an axisymmetric thermal finite element model was used to calculate the temperature distribution in the OTSG during normal operation as well as during MSLB and FWLB transients. Next, axisymmetric finite element analyses were used to establish OTSG tube loads during the transients. Both pressure-induced and thermal-induced loads on the tubes were considered in the structural analysis. The loading conditions corresponding to ΔT that generated the maximum tube axial loading are provided in Table 1-1.

Table 1-1 Loadings at ΔT that generated maximum load

Accident Cond.	Time (min.)	Temperature °C (°F)			Pressure MPa (psi)	
		Downcomer	Steam annulus	Tube	Primary	Secondary
MSLB	20	272 (521)	302 (575)	113 (235)	17.2 (2500)	0
FWLB	1	280 (536)	302 (575)	329 (625)	17.7 (2566)	0.16 (24)

Finite element analysis showed that the axial load on a tube depended on its radial location. Table 1-2 contains the axial loads on two tubes - one located at the center and the other near the outer edge of the tubesheet.

Table 1-2 Calculated axial loads in a tube at the center and outermost tube

Accident Condition	Axial Load, N (lbf)			
	Center		Outermost Tube	
	Mechanical	Mechanical + Thermal	Mechanical	Mechanical + Thermal
MSLB	156 (35)	6263 (1408)	2500 (562)	14000 (3140)
FWLB	214 (48)	-2758 (-620)	2673 (601)	-2535 (-570)

Note that the maximum axial tensile load is 14000 N (3140 lbf), which acts on an outermost tube during MSLB and the total axial load during FWLB is compressive at both locations.

B&W experience with analyses of the OTSGs shows that the two prime contributions to tube loads (and accompanying tube hole dilations) are the "primary pressure-to-secondary pressure differential" and the "tube-to-shell temperature difference". Of these two, the dominant contribution is the "tube-to-shell temperature difference". Therefore, the results of the thermal analysis were post-processed to provide the time-history of the tube-to-shell temperature difference.

The purpose of Reference 4 is to provide a summary of the conservative methods that are used to inspect and disposition the kinetically expanded joints in the original SGs at Three Mile Island, Unit 1. It contains results for MSLB and LOCA. FWLB was not considered because it led to relatively lower tube stresses than MSLB. Two methods were used to calculate the tube axial load – one carried out by GPU Nuclear (GPUN) and the other by FTI.

According to the GPUN methodology, the peak axial tube load of 5827 N (1310 lbf) occurs 60 seconds into the MSLB transient at the periphery of the OTSG. The smallest loads occur at the center of the OTSG tube bundle.

According to the FTI methodology, the results were very similar to the GPUN load results. The peak axial tube load was 5048 N (1135 lbf) at 60 seconds at the OTSG periphery, with the smallest loads at the center as well.

The axial loads computed by both methods appear to be significantly less than those reported in Reference 3.

The acceptance criteria for the circumferential component of volumetric IGA flaws proposed in Reference 5 is based on an allowable length of 16 mm (0.64 in.) or 130 degrees circumference, irrespective of the measured depth. This allowable length is based on tube parting (severance) considerations for an axial load of 14000 N (3140 lbf).

2 ANALYSIS OF OTSG TUBE WITH CIRCUMFERENTIAL DEGRADATION

A single OTSG tube (Fig. 2-1) was considered for analysis. The geometry and properties of the OTSG and tubes assumed in the analyses are given in Table 2-1. The LOCA analysis was conducted earlier than the MSLB analysis and used a slightly different (but inconsequential) geometry. For simplicity, we assumed the TSPs to be uniformly spaced in the vertical direction. In the OTSGs discussed in the previous section, the TSPs were non-uniformly spaced in the vertical direction to provide the highest damping factor and minimize tube vibration.

Table 2-1 Geometry, properties and loadings of the OTSG assumed for analysis

	LOCA	MSLB
Tube Material	Alloy 600 MA	Alloy 600 MA
RT yield stress	359 MPa (52 ksi)	359 MPa (52 ksi)
Tube outer diameter (OD)	15.9 mm (0.625 in.)	15.9 mm (0.625 in.)
Tube wall thickness	1 (0.038 in)	1 (0.038 in)
No. of TSPs	15	15
Distance between top/bottom tubesheet and nearest TSP	1168 mm (46 in)	1067 mm (42 in)
Distance between tube support plates	1016 mm (40 in)	1067 mm (42 in)
Total length of tube	16561 mm (652 in)	17069 mm (672 in)
Tube internal pressure	0	17.2 MPa (2500 psi)
Tube external pressure	-	0
Tube pre-stress	32.4 MPa (4700 psi)	32.4 MPa (4700 psi)
Maximum temperature difference (ΔT) between tube and shell	200-220°C (390°-430°F)	-
Axial load best estimate bounding	-	2891 N (650 lbf) 13344 N (3000 lbf)

Non-linear, finite deformation, elastic-plastic finite element analyses (FEA) were conducted using the code ABAQUS. A total of 34,200 quadratic elements with 153,435 nodes and 40,500 quadratic elements with 179,237 nodes were used for the LOCA and MSLB analyses, respectively. The FWLB case was not analyzed because the literature survey, discussed in section 1, indicated that the stresses due to tube axial loads are either low or compressive and should not challenge the structural integrity of the tubes with circumferential flaws.

Two types of circumferential flaws were considered:

1. A single 100 percent TW or OD part-throughwall (PTW) crack of various lengths
2. Three symmetrically located 100 percent TW or OD PTW wear scars of several lengths and depths (LOCA only).

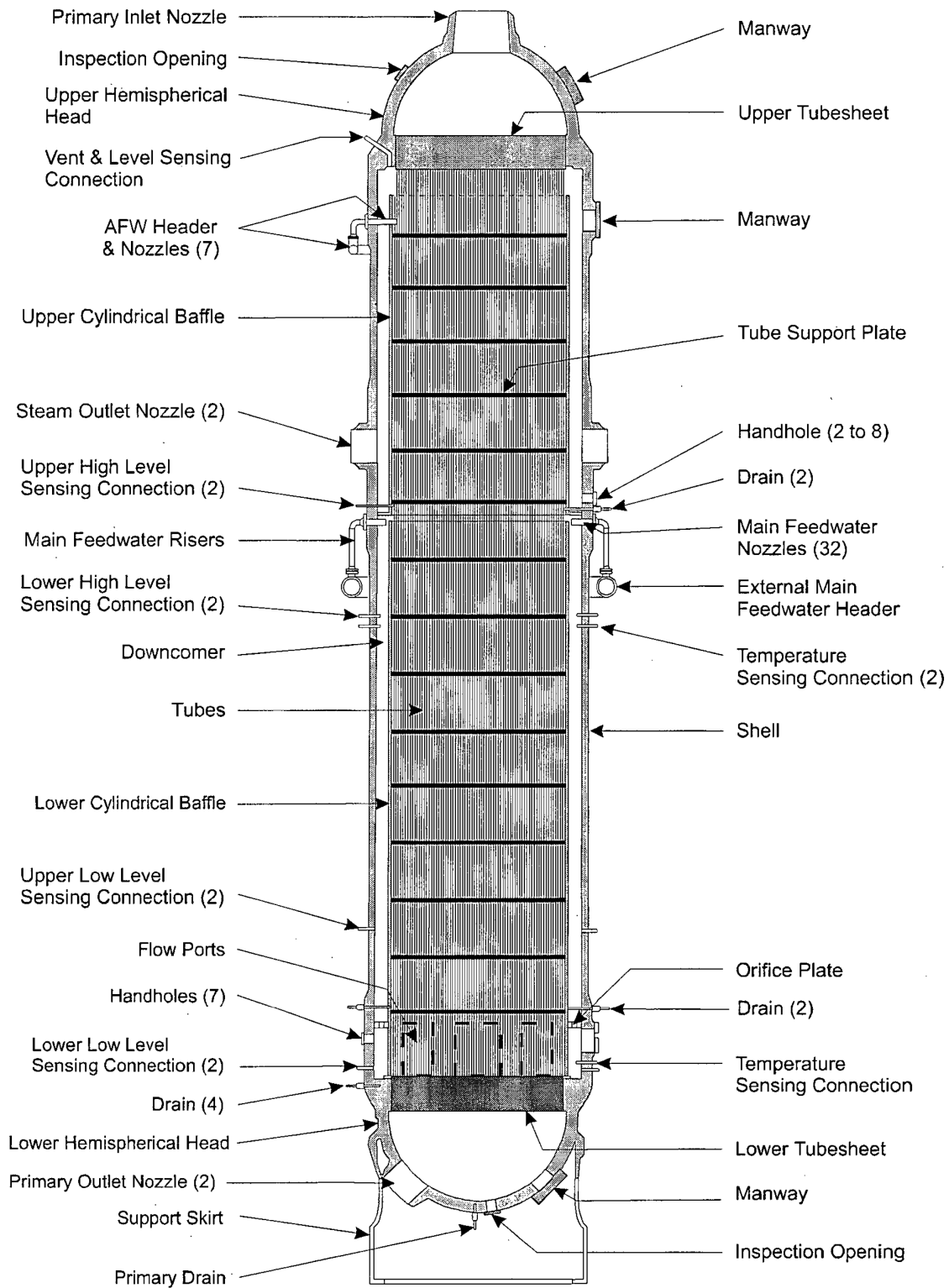


Figure 2-1 Longitudinal cross-section of an OTSG

2.1 Assumptions

- (1) The tube was assumed to be restrained against displacements and rotations at the two ends.
- (2) The crack (or cracks) was (were) placed at the top (or bottom) of the bottom (or top) tubesheet. Although wear marks are normally observed at a high elevation TSP, top (or bottom) of the bottom (or top) tubesheet was considered to be acceptable because of the relatively large length of the tube compared to the distance from the tubesheet to the nearest TSP.
- (3) The loading on the tube was applied by a uniform cooldown temperature after the application of ID and OD pressure, if any.
- (4) To be conservative, the axial load reduction of the tube due to tubesheet bowing was ignored in the case of LOCA analysis.
- (5) Since the peak axial loading on the tube occurs at a relatively low temperature compared to that at the beginning of the accident, room temperature stress-strain curves were used.
- (6) Symmetry was used to reduce the number of degrees of freedom of the problem.

2.2 Loading and Boundary Conditions

The tube was axially constrained at both ends at the tubesheet locations and prevented from lateral displacement at the TSP locations, assuming the tube to slide freely at the tube-to-TSP interfaces. After the application of appropriate pressures, the tube temperature was reduced at a uniform rate keeping the locations of the tubesheet and TSPs fixed. This resulted in an axial tensile loading on the tube.

2.3 Material Properties

Two heats of Alloy 600 were considered, one with yield = 359 MPa (52 ksi) and UTS = 690 MPa (100 ksi) (Heat EX-82-1) and the other with yield = 276 MPa (40 ksi) and UTS = 690 MPa (100 ksi) (Heat NX8520L). The uniaxial engineering and true stress-strain curves for Heats EX-82-1 and NX8520L are shown in Figure 2-2a-b, respectively. The curves were extrapolated along the dotted lines shown in Figure 2-2a-b.

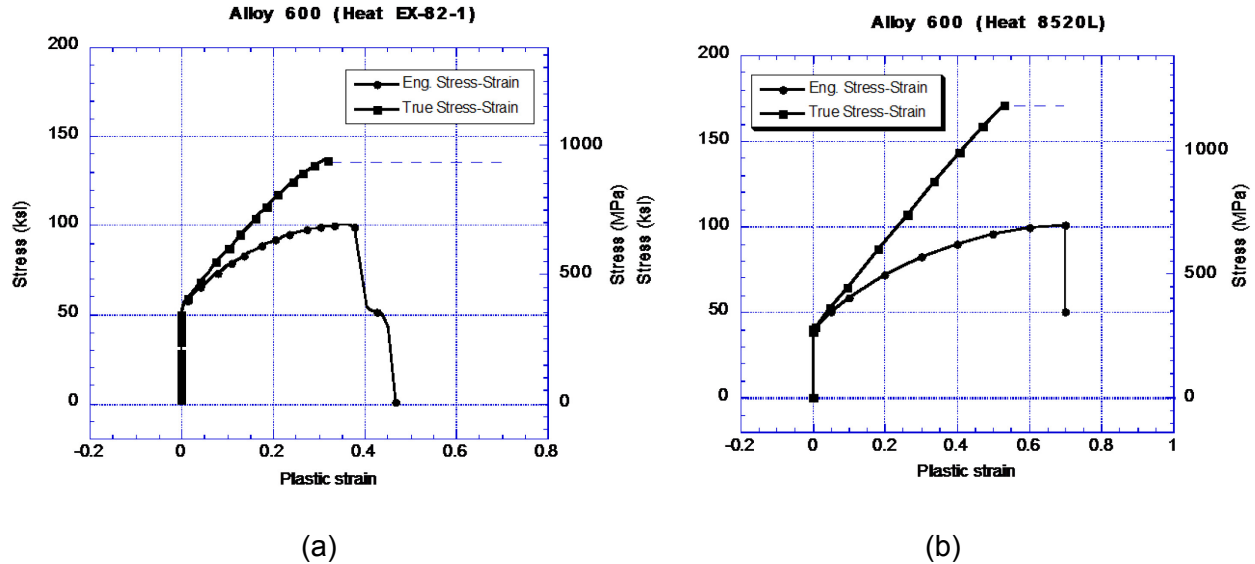


Figure 2-2 Engineering and true stress-strain curves of (a) Alloy 600 Heat EX-82-1 and (b) Alloy 600 Heat NX 8520L

2.3.1 Validation of Finite Element Approach

To partially validate the finite element approach used in the study, the tensile tests of the two heats of Alloy 600 were analyzed in detail. The objective was to verify whether the input true stress-strain curves including their extrapolations can reproduce the uniaxial engineering stress-strain curves up to the peak stress (maximum load). The analyses were carried out with the finite element code ABAQUS using the full non-linear elastic-plastic analysis option. The calculated engineering stress-strain curves (derived from the calculated load vs. displacement curves) are compared with the test data for the two Heats in Figs. 2-3a-b, respectively. The plastic strains at onset of necking (i.e., the uniform elongations) are predicted reasonably well. An alternative way of extrapolating would be to extend the true stress-strain curves smoothly along the final tangent lines in Figs. 2-2a-b. However, such an approach predicted significantly higher plastic strains at onset of necking (i.e., uniform elongations).

2.4 Failure Criteria

2.4.1 Circumferential Cracks

No failure tests were run under the current program. For the tubes with cracks, we used a failure criterion based on critical crack opening displacement (COD), which was originally proposed by Wells (Ref. 9) for materials with high fracture toughness (e.g., Alloy 600) where linear elastic fracture mechanics is inapplicable. The method was further expanded by Burdekin and Stone (Ref. 10) and Rice (Ref. 11) who showed that the critical COD is related to the familiar elastic-plastic plane strain fracture toughness J_{IC} . However, the critical COD criterion does not provide protection from other forms of plasticity-induced failure, such as ductility exhaustion or necking.

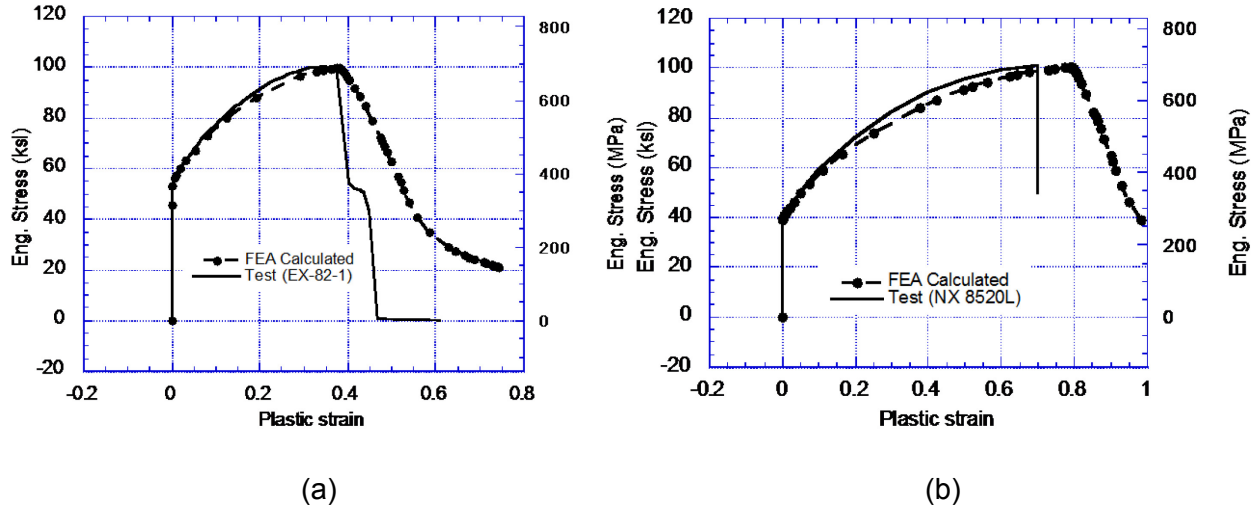


Figure 2-3 Engineering stress-strain curves as measured in uniaxial tensile tests and as predicted by FEA of tensile specimens for Alloy 600 Heats (a) EX-82-1 and (b) NX 8520L

For the current report, the criterion for rupture was selected from the following three criteria, whichever gave the smallest axial load or the lowest critical temperature difference ΔT between the tube and the SG shell:

- (1) Onset of unstable crack tearing when COD equals the remaining ligament thickness, i.e., full wall thickness for 100 percent TW cracks (Fig. 2-4) and radial ligament thickness for PTW cracks (Fig. 2-5). Unstable crack tearing of 100 percent TW cracks usually result in unstable burst but unstable crack tearing of a PTW crack results in a 100 percent TW crack which may not necessarily burst without further increase in ΔT .
- (2) Onset of necking instability (Figure 2-4) when the total axial load reaches a peak value.

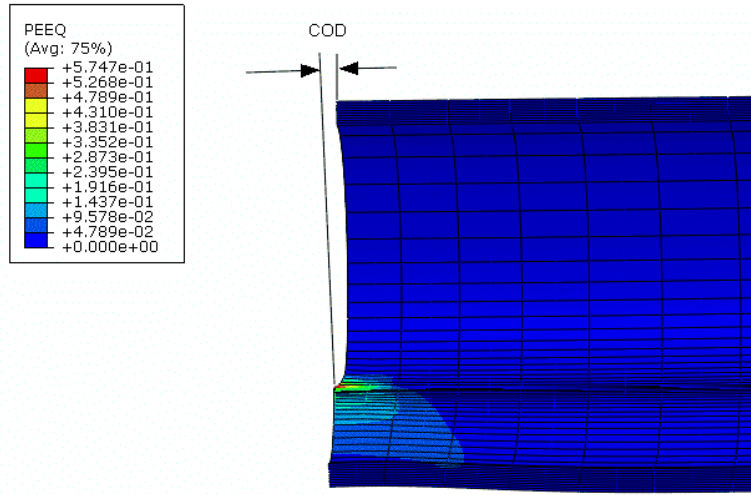


Figure 2-4 Typical crack opening geometry and definition of COD for a 100 percent TW crack

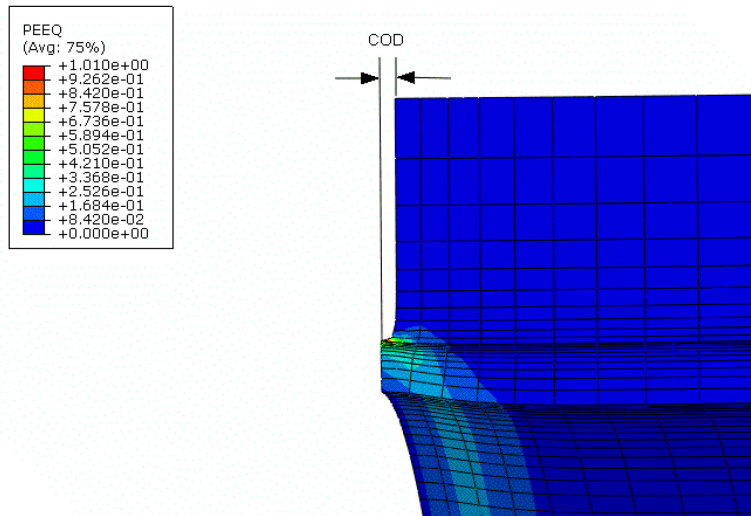


Figure 2-5 Typical crack opening geometry and definition of COD for a PTW crack

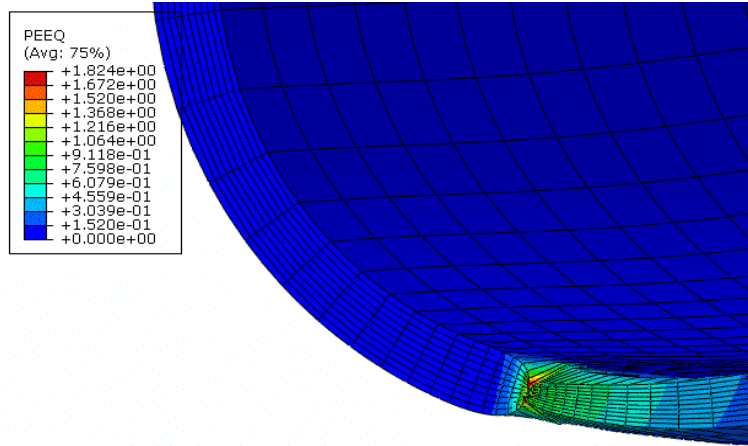


Figure 2-6 Typical necking initiation in a specimen with 100 percent TW crack

- (3) Onset of tensile cracking initiation occurs when the average equivalent plastic strain averaged over all the crack tip elements through the thickness equals the ductility limit (assumed = 100 percent). The typical size of the crack tip element varied in length between $5\ \mu\text{m}$ (2×10^{-4} in.) and $10\ \mu\text{m}$ (4×10^{-4} in), which are of the order of a grain size of the material.

2.4.2 Wear Marks

2.4.2.1 Wear Mark vs. EDM Slot

Neither the J_{IC} nor the critical COD criterion is directly applicable to wear marks, which, strictly speaking, are not cracks. Results from burst tests on Alloy 600 tubes with axial rectangular slots and elliptical wastage were published by Alzheimer et al. in NUREG/CR-0718 (Ref. 12). The test burst pressures of tubes with elliptical wastage depended primarily on the depth of the flaw. On the other hand, the burst pressures of axial slots depended both on the slot length and the depth. A comparison of burst pressures of tubes with PTW axial slots and elliptical wastage of equal depths showed that, in general, their magnitudes are comparable. The burst pressures of EDM slots with lengths equal to or less than the radius of the tube are greater than the burst pressures of elliptical wastage with the same depth and vice versa for axial slots with lengths greater than the radius of the tube.

Under the auspices of Ontario Power Generation (Canada), burst tests were conducted in triplicate on 25 mm (1 in) long, 75 percent deep axial EDM notches and square slots simulating wear marks in Inconel 600, Incoloy 800 and Monel 400 tubes (Refs. 13, 14). Based on the eighteen tests (3×3×2) the difference in failure pressure between the two defects (in a given tube) is not significant; on average the axial EDM notch has a failure pressure that is 3 percent higher than the square slot. This is not significant compared to the test-to-test variability.

Since the available rupture tests of tubes with wear marks and wastage showed that the behavior of PTW wear marks and PTW slots of the same depth are similar, we used the same critical COD failure criteria for wear marks that we used for cracks (section 2.4.1).

3 RESULTS FOR LOCA ANALYSES

The results presented here are for a material with 359 MPa (52 ksi) yield stress. A review of the properties of the MA Alloy 600 tubes showed that the assumed value of the yield stress is within the scatter bound of yield stresses of alloy 600 tubes of all diameters, although slightly on the higher side. Since in most cases a critical COD criterion or a critical crack tip plastic strain criterion controls failure and the stress is deformation-controlled thermal stress, the results are relatively insensitive to a change in yield stress.

3.1 Single Circumferential Cracks

3.1.1 Single 100 Percent Throughwall Circumferential Crack

Figure 3-1 shows a plot of the variation of crack opening displacement (COD) with the temperature difference ΔT for a number of 100 percent TW cracks with various lengths. The critical temperature differences for the various cracks are obtained from the curves at the critical COD value of 0.97 mm (0.038 in). The critical COD for crack tearing is equal to the wall thickness. To check whether failure by onset of necking is possible before onset of unstable crack tearing, the variation of COD for these cracks are plotted against total axial load in Fig. 3-2. Note that none of the curves reaches peak load prior to reaching the critical value of the COD, indicating that necking will not occur in any of these cracks prior to onset of unstable crack tearing. In a similar fashion, the variation of the crack tip equivalent plastic strain through the wall thickness for the various cracks at the critical ΔT s are plotted in Fig. 3-3. In all cases, the peak values of the crack tip equivalent plastic strain are less than the ductility limit of 100 percent, thus indicating that tensile crack initiation will not occur prior to onset of unstable crack tearing.

Results from all the analyses are plotted in Fig. 3-4 as a critical temperature difference ΔT vs. crack length plot. Note that the critical crack length corresponding to the $\Delta T=220^\circ\text{C}$ (428°F) for LB LOCA is $\sim 110^\circ$. Thus, any 100 percent TW crack longer than 110° is predicted to fail during the LB LOCA loading. For comparison, a recent submittal by AREVA with regard to LB LOCA analysis of Davis Besse reported that the 50/50 limit for a 100 percent TW circumferential crack is 14 mm (0.55 in) (107°) (Ref. 8).

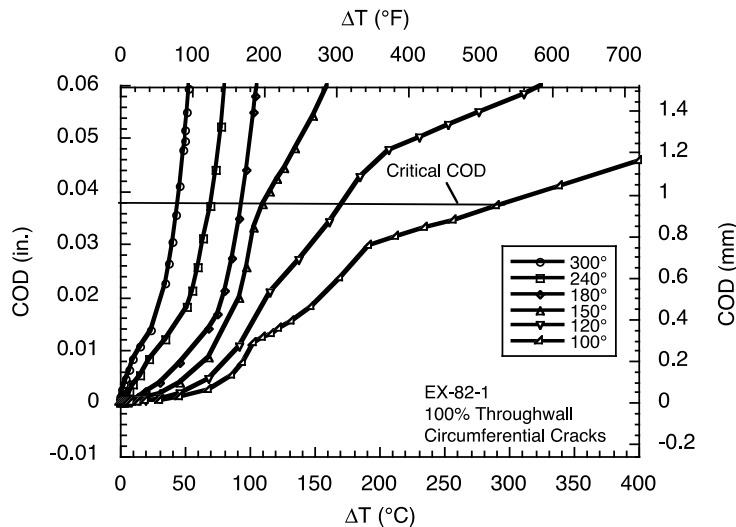


Figure 3-1 Variation of COD with ΔT for 100 percent TW cracks of various lengths

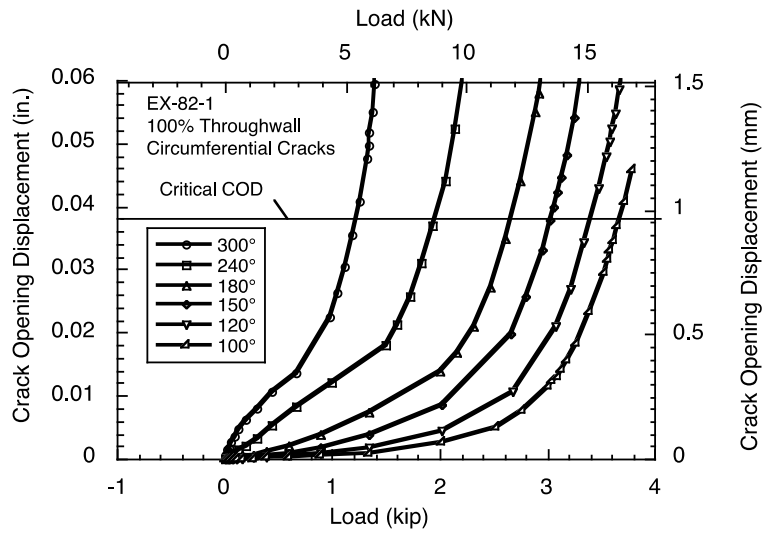


Figure 3-2 Variation of COD with total axial load for 100 percent TW cracks of various lengths

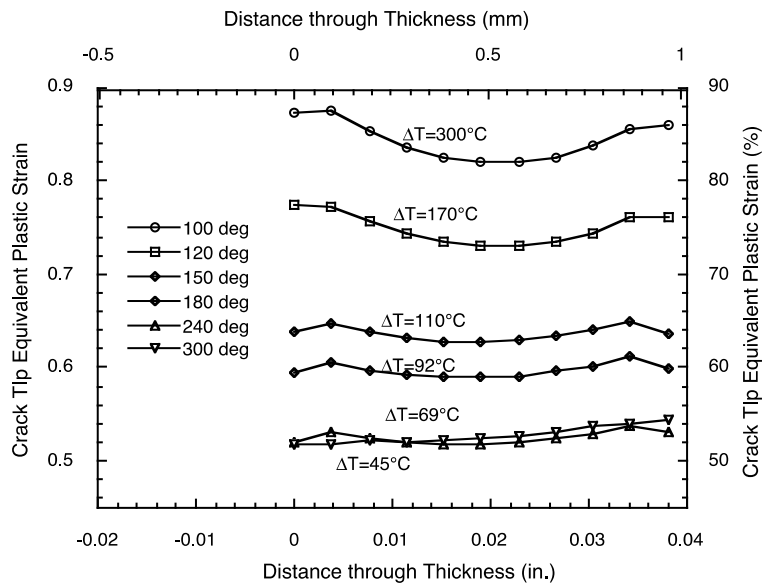


Figure 3-3 Variation of peak crack tip equivalent plastic strain through the wall thickness at the critical temperature differences ΔT s for the various cracks obtained from Fig. 3-1

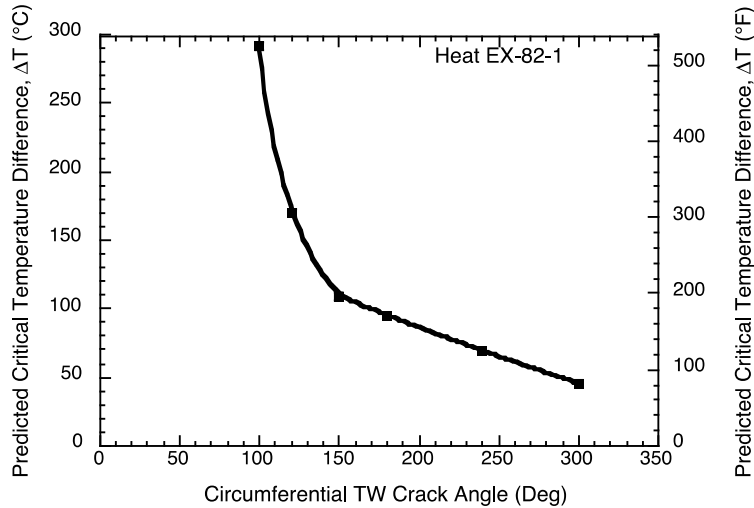


Figure 3-4 Variation of critical temperature difference ΔT with 100 percent TW circumferential crack length

3.1.2 Part-Throughwall 360° Crack

Variations of COD and peak equivalent plastic strain at the crack tip of a PTW 360° circumferential crack with temperature difference ΔT are shown in Figs.3-5 and 3-6, respectively. The COD values are too low to cause unstable cracking of the remaining ligament at the crack tip up to the ΔT values shown in Fig. 3-5. The critical temperatures for tensile cracking initiation can be obtained from Fig. 3-6 as the ΔT values when the peak equivalent plastic strain at the crack tip equals the ductility limit, 100 percent. The variation of the critical temperatures with the 360° crack depth predicted by various theories are plotted in Fig. 3-7. The critical temperatures predicted by the simple net section flow theory are close to those predicted by the tensile rupture initiation model. The unstable cracking model predicts significantly larger critical temperature ΔT . The tensile rupture initiation model predicts that any 360° crack shallower than 31 percent deep will survive the LBLOCA loading. The net section flow theory predicts the critical depth to be 38 percent. For comparison, the Electric Power Research Institute (EPRI) guideline for SG Integrity Assessment (using percent degraded area, PDA) predicts the critical depth to be 42 percent (Ref. 15).

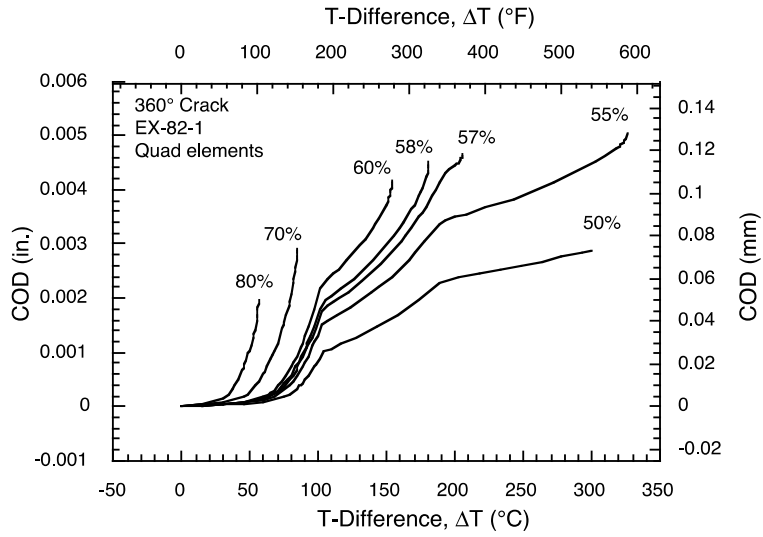


Figure 3-5 Variation of COD of 360° PTW cracks of various depths with temperature difference ΔT

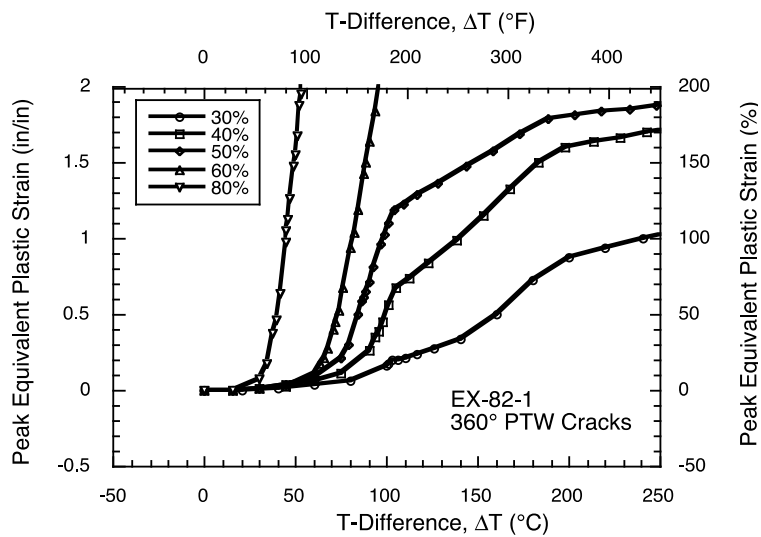


Figure 3-6 Variation of peak equivalent plastic strain at the crack tip of 360° PTW cracks of various depths with temperature difference ΔT

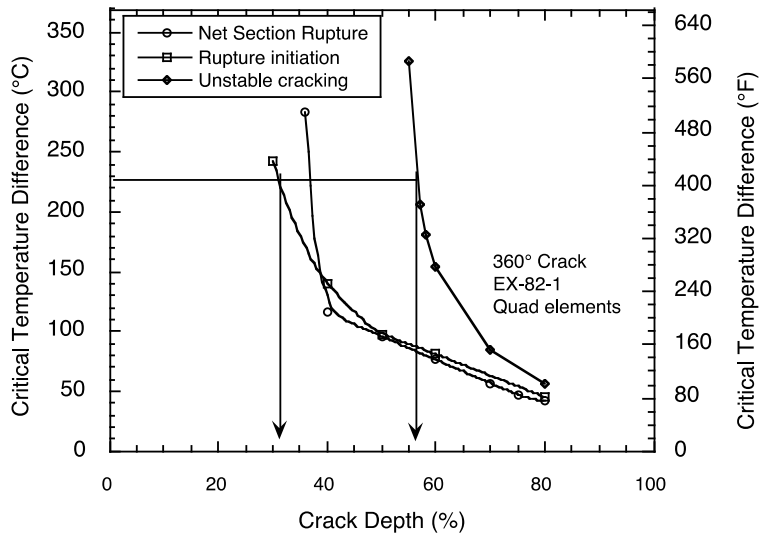


Figure 3-7 Variations of critical temperature difference with crack depth of 360° circumferential PTW cracks predicted by various failure criteria

3.1.3 Single Part-Throughwall Cracks (<360°)

The predicted temperature for ligament rupture of each crack is determined by first calculating two critical failure temperatures, one corresponding to unstable crack tearing (COD = remaining crack tip ligament thickness) and the other corresponding to crack tip rupture initiation mechanism (average through-thickness crack tip equivalent plastic strain = 100 percent). The lower of the two calculated critical temperatures is the predicted value of the temperature for ligament rupture of that crack.

3.1.3.1 Single 90 Percent Deep PTW Cracks

Figure 3-8 shows the variation of COD with temperature difference ΔT for single 90 percent deep 30°, 60°, 120° and 300° PTW circumferential cracks. The critical temperature difference for ligament rupture by unstable crack tearing corresponds to COD = 1 mm (0.038 in), which is attained by a 300° crack at $\Delta T = 55^\circ\text{C}$ (130°F), by a 120° crack at 70°C (158°F), by a 60° crack at 140°C (284°F) and by a 30° crack at $>300^\circ\text{C}$ (572°F).

Variations of the peak crack tip equivalent plastic strain along the crack front of 90 percent deep, 300°, 120°, 60°, and 30° PTW circumferential cracks are plotted in Figs 3-9a-d, respectively. The critical temperature difference for failure by rupture initiation at the crack tip (i.e., average equivalent plastic strain = 100 percent) is attained by a 300° crack at $\Delta T = 70^\circ\text{C}$ (158°F), by a 120° crack at 74°C (167°F), by a 60° crack at 124°C (256°F) and by a 30° crack at 296°C (556°F). Except for the 300° and 120° cracks (Fig. 3-9a-b), all the rest of the cracks are predicted to fail by crack tip rupture initiation. The rupture temperatures noted in the figures correspond to an average equivalent plastic strain at the crack tip of 100 percent. The failure of the 300° and 120° cracks are predicted to be due to onset of unstable crack tearing (Fig. 3-8).

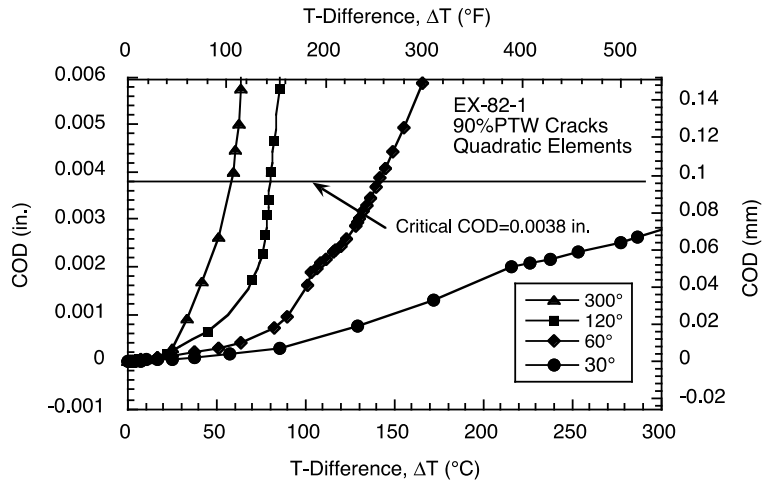


Figure 3-8 Variation of COD of 90 percent deep PTW cracks of various lengths with temperature difference ΔT

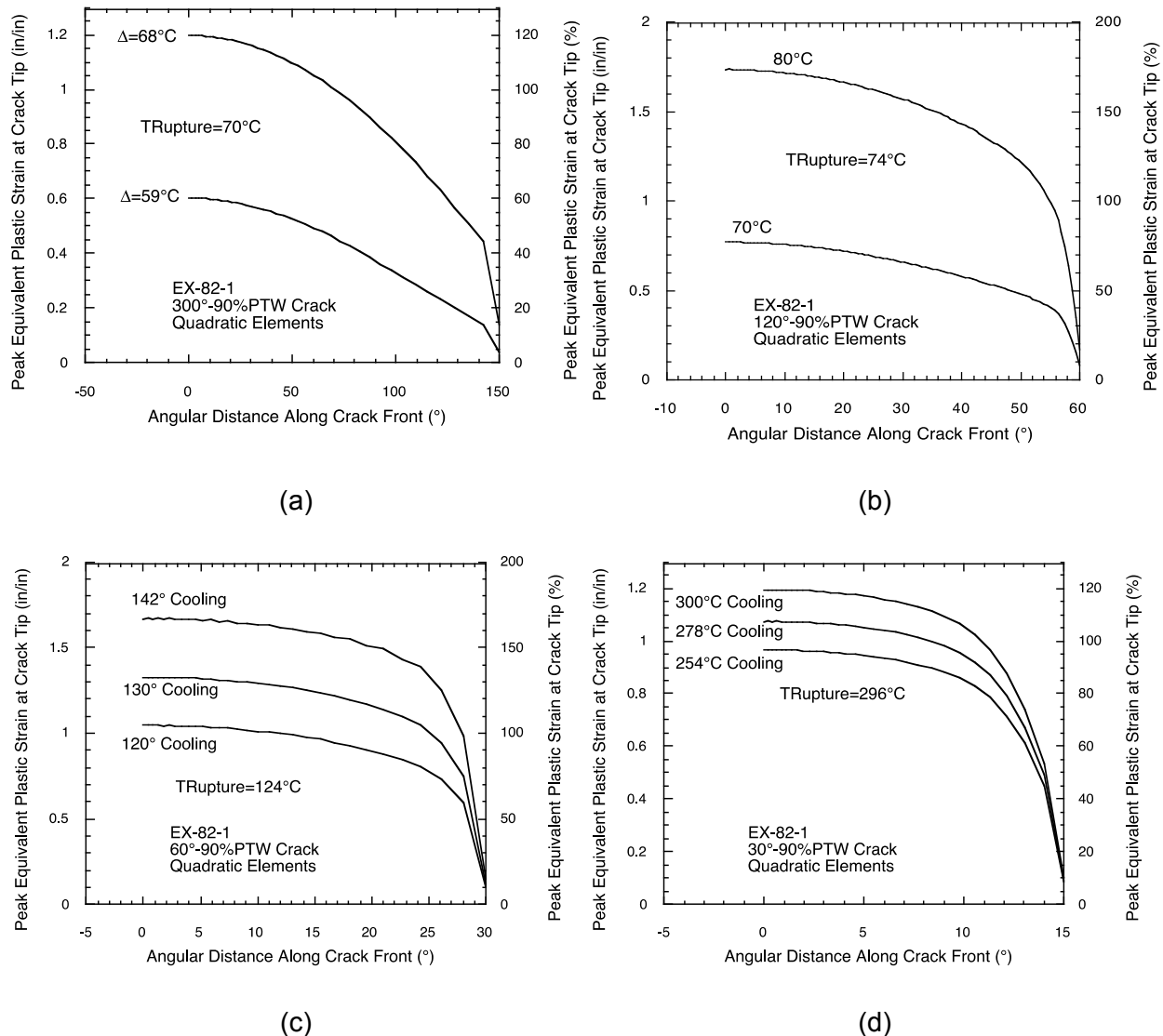


Figure 3-9 Variation of peak equivalent plastic strain at the crack tip along the crack front of 90 percent deep (a) 300°, (b) 120°, (c) 60° and (d) 90° cracks

3.1.3.2 Single 80 Percent Deep PTW Cracks

Figure 3-10 shows the variation of COD with temperature difference ΔT for single 80 percent deep 50°, 60°, 90°, 120° and 180° PTW circumferential cracks. The critical temperature difference for unstable crack growth for ligament rupture corresponds to COD = 1.9 mm (0.0076 in), which is attained by a 50° crack at $\Delta T = 325^\circ\text{C}$ (580°F). However, all the cracks fail by tensile rupture initiation at the crack tip at ΔT s smaller than the maximum ΔT s attained in Fig. 3-10, as discussed below.

Variations of the peak crack tip equivalent plastic strain along the crack front of the 80 percent deep, 50°, 90°, 120° and 180° PTW circumferential cracks are plotted in Figs 3-11a-d, respectively. The rupture temperatures noted in the figures correspond to an average equivalent plastic strain at the crack tip of 100 percent. All of the cracks are predicted to fail by rupture initiation at the crack tip.

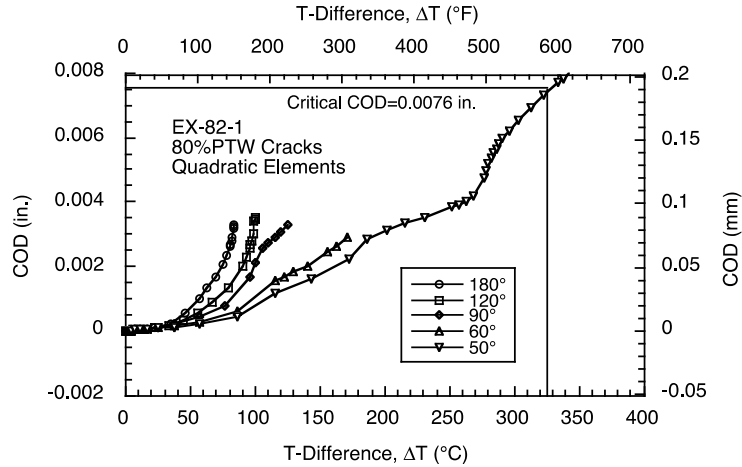


Figure 3-10 Variation of COD of 80 percent deep PTW cracks of various lengths with temperature difference ΔT

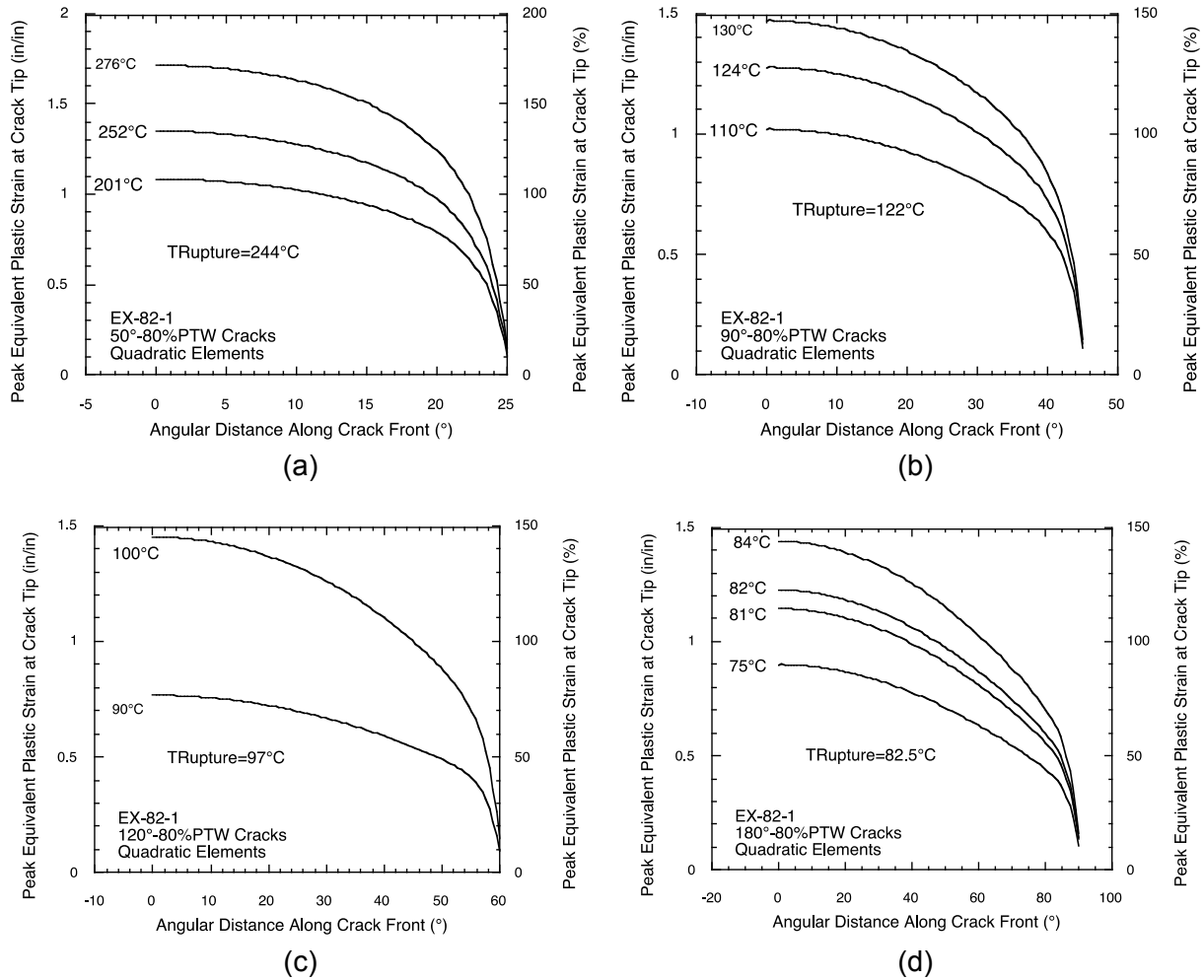


Figure 3-11 Variation of peak equivalent plastic strain at the crack tip along the crack front of 80 percent deep (a) 50°, (b) 90°, (c) 120° and (d) 180° cracks

3.1.3.3 Single 60 Percent Deep PTW Cracks

A plot of COD vs. temperature difference ΔT for 60 percent deep 120°, 180°, and 240° circumferential PTW cracks are plotted in Fig. 3-12. In reality, all the cracks shown in the figure fail by tensile rupture initiation at the crack tips prior to the maximum ΔT s shown in Figure 3-12.

Variations of the peak crack tip equivalent plastic strain along the crack front of 60 percent deep, 240°, 180° and 120° circumferential cracks are plotted in Figs 3-13a-c, respectively. The rupture temperatures noted in the figures correspond to an average equivalent plastic strain at the crack tip of 100 percent. All of the cracks are predicted to fail by rupture initiation at the crack tip.

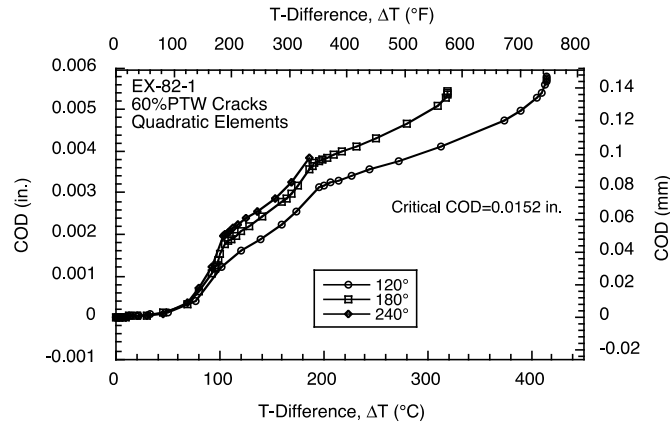


Figure 3-12 Variation of COD of 60 percent deep 120°, 180°, and 240° PTW cracks of various lengths with temperature difference ΔT

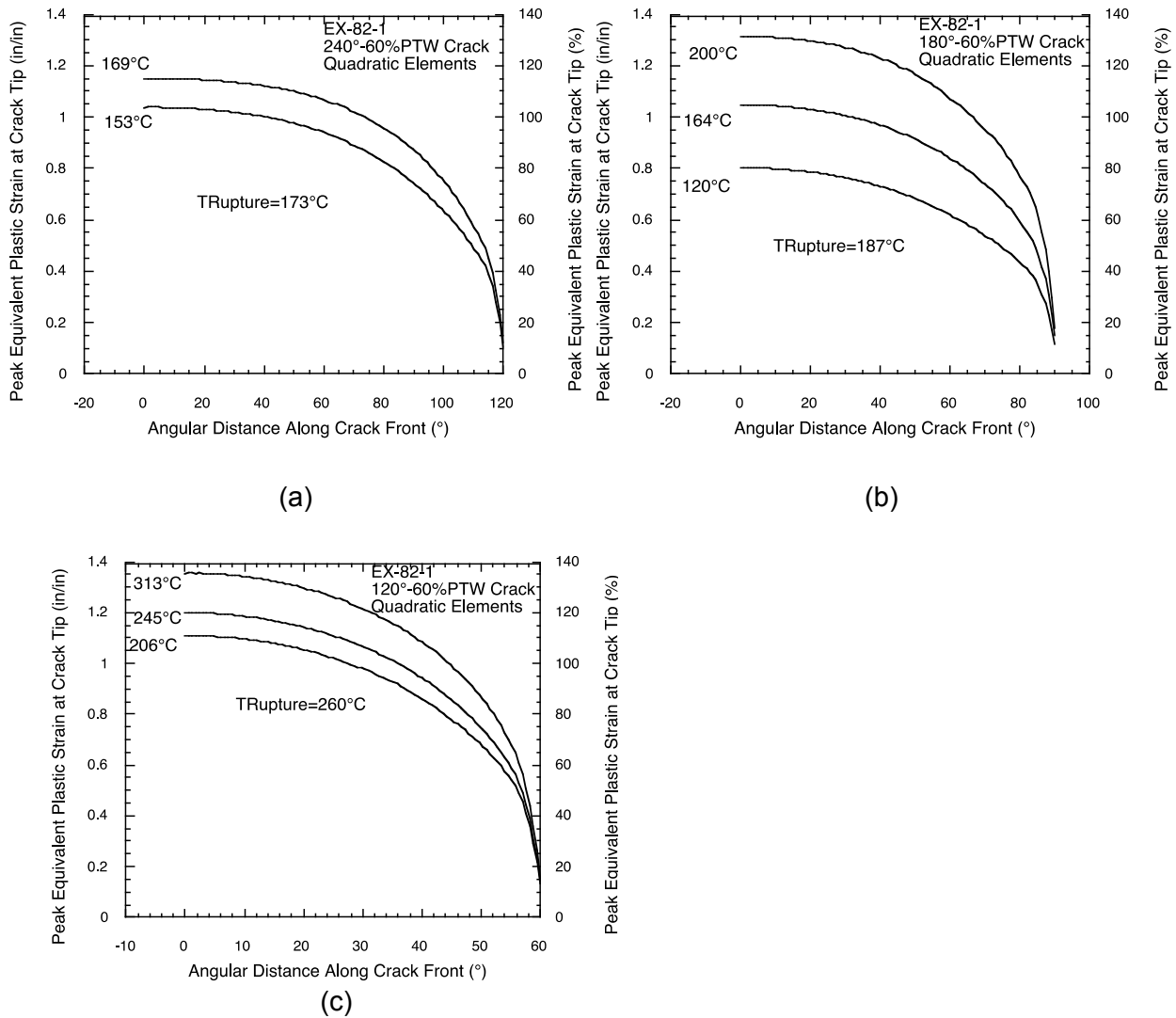


Figure 3-13 Variation of peak equivalent plastic strain at the crack tip along the crack front of 60 percent deep (a) 240°, (b) 180°, and (c) 120° cracks

3.1.4 Failure Diagram for Single Circumferential Cracks

All of the failure temperature data are summarized in the failure diagram (Fig. 3-14). The open symbols in Fig. 3-14 represent crack tip ligament rupture without unstable burst of the tube. The filled symbols represent ligament rupture followed immediately by unstable burst of the tube. Note that any 60 percent deep crack shorter than 140° is predicted to survive the 220°C (428°F) temperature difference during the LBLOCA without ligament rupture or unstable burst. Similarly, any 80 and 90 percent deep crack shorter than 55° and 40°, respectively is predicted to survive the LBLOCA transient.

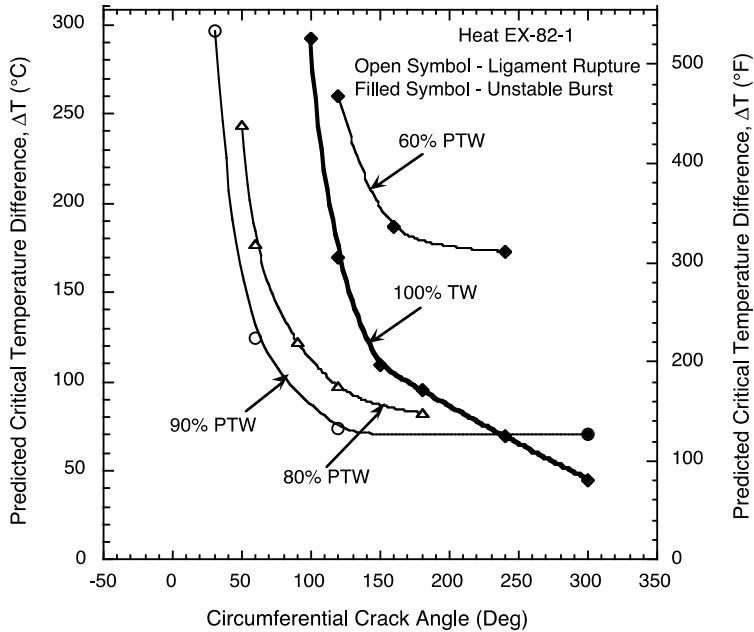


Figure 3-14 Variations of failure temperatures of 60, 80, 90 percent PTW and 100 percent TW circumferential cracks with crack angle

All of the failure data have been combined into a failure map, shown in Fig. 3-15, for the failure of a 16 mm (5/8 in.) diameter SG tube with a single PTW circumferential crack subjected to $\Delta T=220^{\circ}\text{C}$ (428°F) during the LBLOCA. The map identifies three zones of failure mechanisms depending on the crack angle and crack depth. They are (1) a zone of no leakage or unstable burst, (2) a zone of leakage without unstable burst and (3) a zone of unstable burst.

3.2 Wear Marks at Trefoil TSPs

Since the length of each of the three lands in a typical trefoil TSP is 4 mm (0.16 in.), the circumferential extent of each contact area is $\sim 30^{\circ}$. However, there is a possibility that, after initiating, some of the wear marks may extend in the circumferential direction during service. Therefore, we analyzed the potential rupture of $3 \times 30^{\circ}$ as well as $3 \times 45^{\circ}$ wear marks located symmetrically around the circumference of the tube. From symmetry, we needed to analyze only a 60° circumferential slice of the tube, 16.6 m (652 in.) long, containing half of a wear mark.

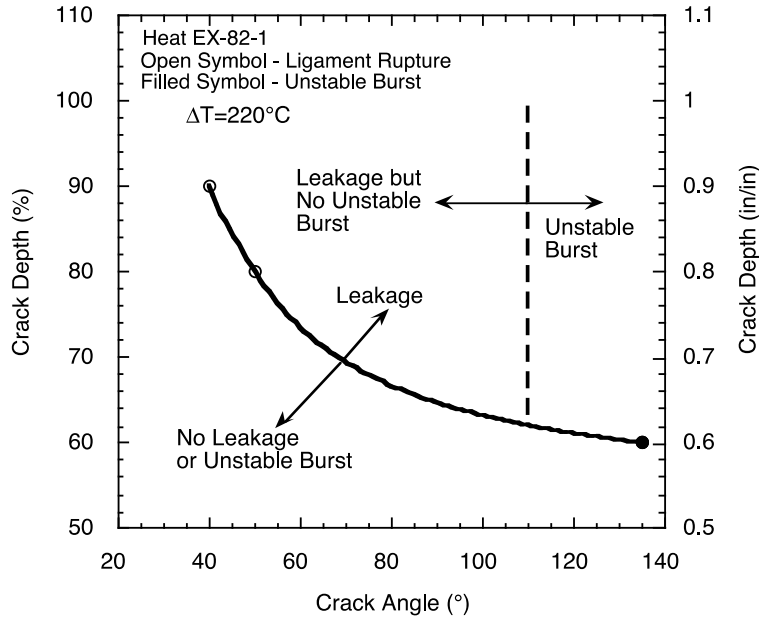


Figure 3-15 Failure map of a circumferential crack in a 15.9 mm (5/8 in.) diameter SG tube subjected to LBLOCA cooldown loading

As discussed in section 2.4.2, we used the same criteria for the rupture of wear marks that we used for cracks (see Section 2.4.1), i.e., we determined the failure load or temperature rise using the following three criteria and used whichever gave the lowest load or temperature rise:

- (1) Onset of unstable crack tearing when COD equals the remaining ligament thickness. For 100 percent TW cracks, the COD associated with unstable crack tip tearing is the wall thickness of the tube, whereas for PTW cracks, it is the remaining crack tip radial ligament thickness.
- (2) Onset of necking instability when the total axial load reaches a peak value.
- (3) Onset of tensile cracking initiation when the average equivalent plastic strain, averaged over all the crack tip elements adjacent to the entire crack front, equals the ductility limit (assumed = 100 percent).

3.2.1 Part-Throughwall OD Wear Marks

The wear marks (60 and 90 percent deep) are spaced 120° apart circumferentially. As discussed earlier, from symmetry, we need to analyze only a 60° circumferential slice of the 16.6 m (652 in.) long tube. For the $3 \times 45^\circ$ wear marks, each slice consists of a 22.5° circumferential wear mark (60 or 90 percent deep) with a 37.5° full thickness circumferential ligament. Similarly, for the $3 \times 30^\circ$ wear marks, the slice consists of a 15° circumferential wear mark (60 or 90 percent deep) with a 45° full thickness circumferential ligament.

Figures 3-16a-b show the variation of the COD with temperature difference ΔT for the 60 and 90 percent deep wear marks, respectively. The $3 \times 30^\circ \times 90$ percent deep wear marks are predicted to experience the onset of unstable crack tip ligament tearing at a ΔT of 280°C (536°F) and the $3 \times 45^\circ \times 90$ percent deep wear marks are predicted to experience the onset of unstable crack tip ligament tearing at a ΔT of 140°C (268°F). By interpolation, the longest individual length of 3×90

percent deep wear marks that will not fail during the LBLOCA ($\Delta T=220^{\circ}\text{C}$) by onset of unstable crack tip tearing is predicted to be 36° . The temperature differences for unstable crack tip ligament tearing of both ($3\times 30^{\circ}$ and $3\times 45^{\circ}$) 60 percent deep wear marks are predicted to be much higher ($>300^{\circ}\text{C}$) than what would be experienced during an LBLOCA.

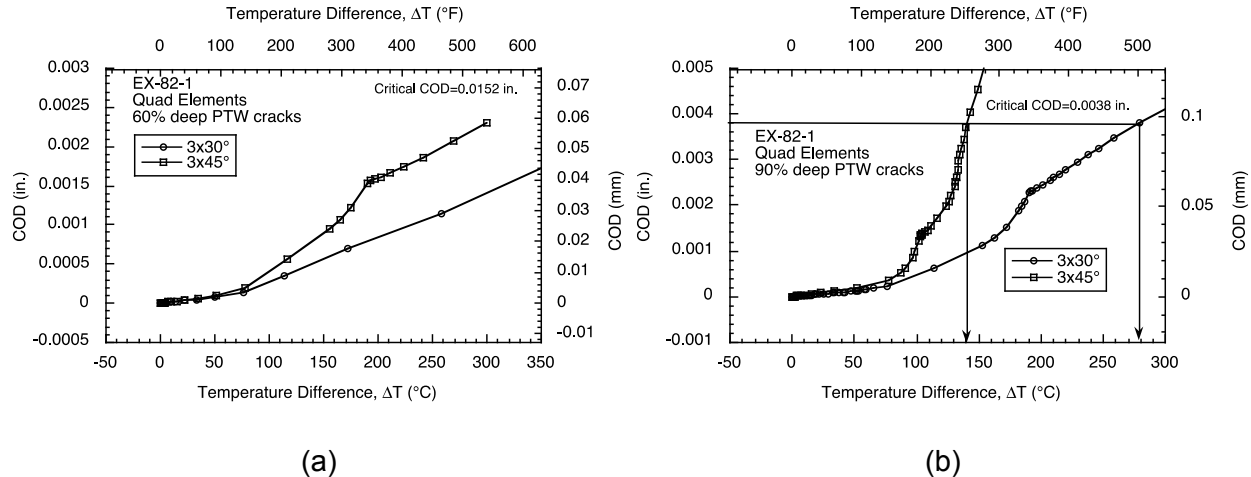


Figure 3-16 Variation of the COD of (a) 60 and (b) 90 percent deep $3\times 30^{\circ}$ and $3\times 45^{\circ}$ PTW wear marks with temperature difference ΔT

Plots of the angular variation of the equivalent plastic strains along the crack tip at various ΔT s are shown for the 90 percent deep (a) $3\times 30^{\circ}$ and (b) $3\times 45^{\circ}$ wear marks in Figs. 3-17a-b, respectively. The average effective plastic strain along the entire crack tip of the 90 percent deep wear marks equals the ductility limit of 100 percent at $\Delta T = 133^{\circ}\text{C}$ (271°F) for the $3\times 45^{\circ}$ wear marks and 207°C (405°F) for the $3\times 30^{\circ}$ wear marks. The peak crack tip effective plastic strains of the 60 percent deep wear marks in both cases are less than the ductility limit even at a temperature difference (ΔT) of 300°C (572°F) during the LBLOCA transient.

To check whether the crack tip ligaments of the 90 percent deep $3\times 30^{\circ}$ and $3\times 45^{\circ}$ wear marks experience necking, the loads carried by the crack tip ligaments and the solid full thickness ligaments are plotted in Fig. 3-18a-b, respectively. The peak at 191°C was taken as at the horizontal tangent location. Remeshed refers to a refined mesh at which the solution converged. Note that although the loads carried by the crack tip PTW ligaments reach peak values at 191°C (376°F) and 128°C (262°F), respectively, the total loads continue to rise even after the PTW ligament loads reach their peak values. The loads shed by the crack tip PTW ligaments are transferred to the full thickness ligaments. Thus, the whole system remains stable (no unstable rupture) even though under a purely load-control situation (the current loading is approximately displacement-control) the crack tip ligament would have failed unstably by necking.

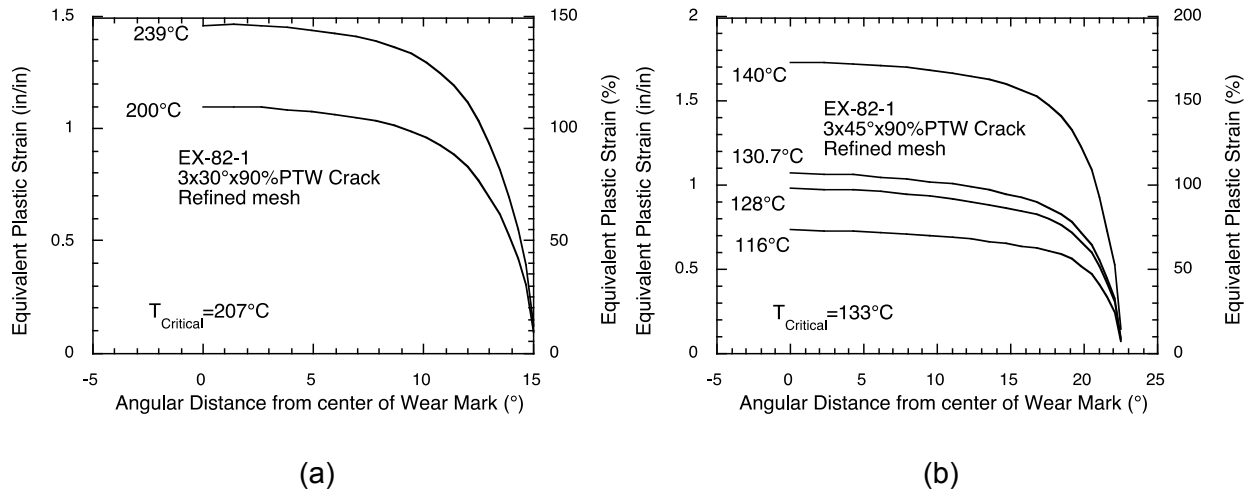


Figure 3-17 Variation of the equivalent plastic strain along the crack tip of the 90 percent deep (a) 3x30° and (b) 3x45° wear marks with angular distance at various values of ΔT

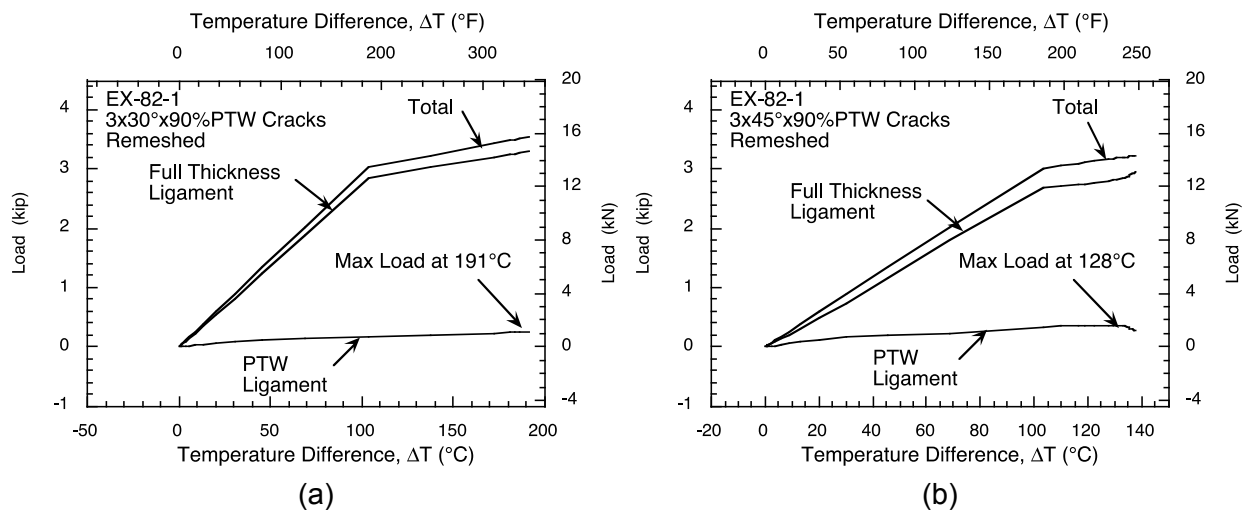


Figure 3-18 Variation of the loads carried by the crack tip PTW ligament, the solid full thickness ligament and the total load with ΔT for (a) 3x30°x90 percent and (b) 3x45°x90 percent PTW cracks

3.2.2 100 Percent Throughwall Wear-Induced Cracks

Whether a PTW wear mark remains stable after ligament rupture or whether it undergoes unstable burst depends on the stability of the 100 percent TW crack which forms after ligament rupture. Therefore, we analyzed the case of 100 percent TW 3x45° cracks by FEA.

The variations of COD with temperature difference ΔT and axial load are plotted in Figs. 3-19a-b, respectively. The maximum COD during the LB LOCA is ≈ 0.25 mm (0.01 in.), which is much less than the critical COD, 1 mm (0.038 in.). Therefore, the 100 percent TW crack will not experience initiation of unstable tearing failure during LB LOCA. Thus, even if the PTW wear mark ligament were to rupture and create a 100 percent TW crack, it would remain stable. Also, since Fig. 3-19b shows that the load does not reach a peak value (i.e., maximum beyond which

it decreases) up to a ΔT of 400°C (752°F), the full-thickness ligaments between the cracks will not experience onset of necking during LB LOCA.

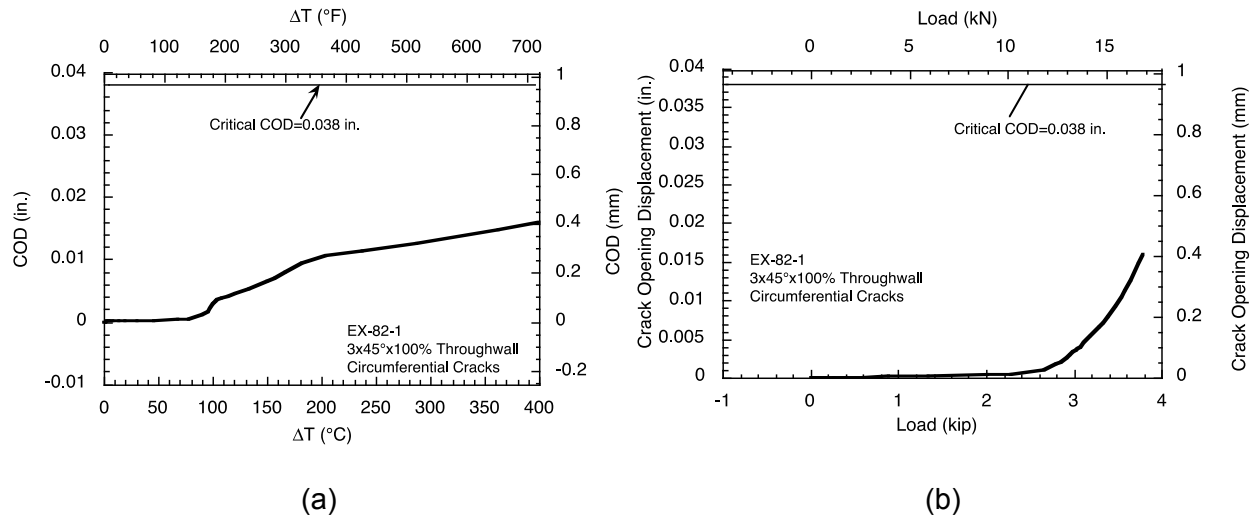


Figure 3-19 Variation of the COD with (a) temperature difference ΔT and (b) load for 100 percent TW 3x45 cracks. Also shown are lines representing the critical COD for the initiation of unstable tearing

Plots of the thickness-averaged equivalent plastic strains in four crack tip elements (out of ten) at one of the 3x45°x100 percent TW crack tips of the tube vs. ΔT are shown in Fig. 3-20. For reference, the average size of the crack tip elements is 75 μm (0.003 in.), which is of the order of several grain size for this material. Since the four curves are close to each other, the distribution of plastic strain at the crack tip through the thickness of the tube is quite uniform. The average effective plastic strain at the crack tip reaches the ductility limit of 100 percent at $\Delta T = 350^\circ\text{C}$ (662°F), which is significantly greater than the maximum ΔT expected during LB LOCA. Therefore, the cracks will not experience initiation of tensile crack growth by the mechanism of exhaustion of ductility during LB LOCA. For reference, the critical temperature (ΔT) for the 100 percent TW 3x45° cracks predicted by the net section rupture theory is 280°C (536°F).

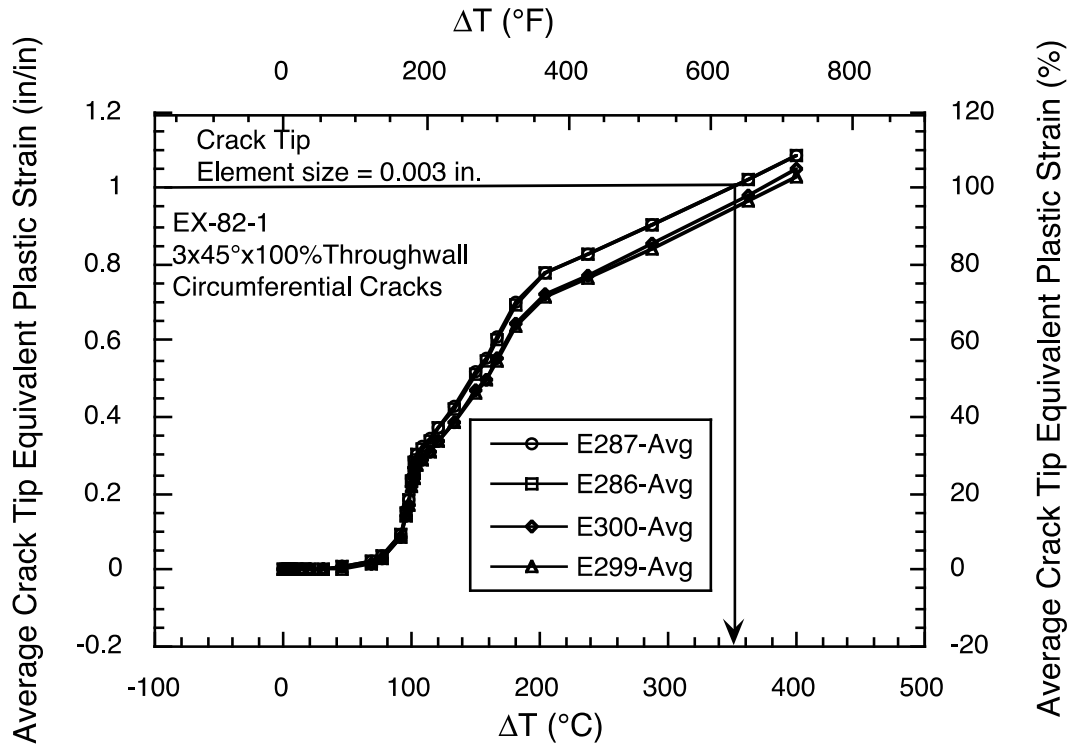


Figure 3-20 Variation of the average equivalent plastic strain in four elements at the crack tip of 100 percent TW 3x45° cracks with ΔT

3.2.3 Summary of Results for Wear Marks

Based on the results, it is predicted that the 60 percent deep 3x30° and 3x45° PTW wear marks will survive LB LOCA without ligament rupture or unstable burst. The 90 percent deep 3x30° and 3x45° PTW wear marks are predicted to suffer crack tip ligament rupture and become 100 percent throughwall flaws at $\Delta T = 207^\circ\text{C}$ (405°F) and $\Delta T = 133^\circ\text{C}$ (271°F), respectively. By extrapolation, the longest individual length of 3x90 percent deep wear marks that will survive the LB LOCA cooldown ($\Delta T = 220^\circ\text{C}$ [428°F]) without ligament rupture is 27.5°.

Based on the results for the 100 percent throughwall 3x45° cracks, it is predicted that neither the 90 percent PTW 3x30° wear marks nor the 90 percent PTW 3x45° wear marks will experience unstable burst after ligament rupture during the LB LOCA cooldown.

For comparison, submittal by AREVA with regard to LB LOCA analysis of Davis Besse cites experimental data that show wear scar depth has to be >92 percent deep for it to pop through (i.e., experience ligament rupture, Ref. 7). Also, 100 percent deep wear scars can meet LB LOCA structural integrity requirement at 95/50 confidence. Also, AREVA has reported with regard to LB LOCA analysis of TMI-1 that the allowable pop-through depth for a TSP wear scar is 78 percent through-wall and that the ligament pop-through will not lead to a tube "burst" (Ref. 8).

4 RESULTS FOR MSLB

4.1 Single 100 Percent Throughwall Circumferential Flaw

A series of analyses for 150°, 180°, 240°, 270° and 330° long 100 percent throughwall cracks was completed. Variations of the COD with axial load for these flaws are plotted in Fig. 4-1. Since the critical COD = 0.97 mm (0.038 in.), 100 percent TW cracks >150° will experience unstable tearing due to the bounding axial load 13,344 N (3000 lbf). A 330° crack is predicted to fail at the best estimate tube axial load 2891 N (650 lbf). Cracks >330° should reach the critical COD (i.e., fail) prior to reaching best estimate tube axial load 2891 N (650 lbf).

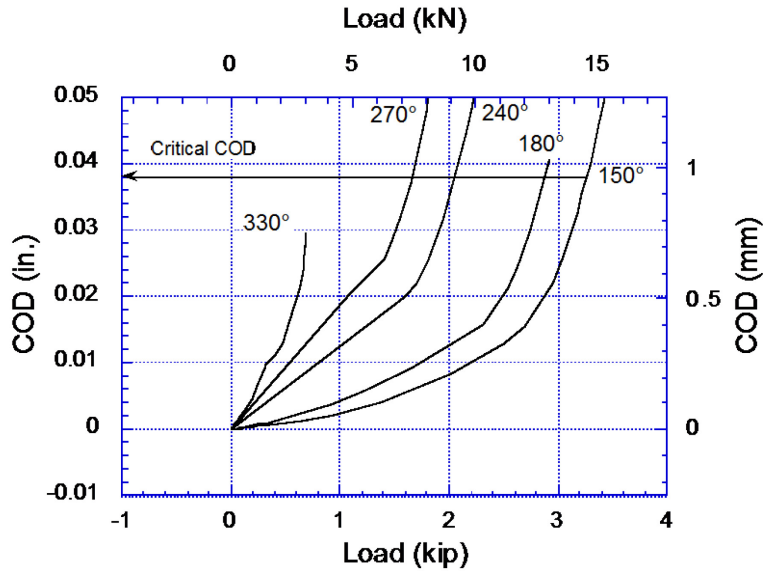


Figure 4-1 Variation of COD with axial load for various 100 percent TW cracks

4.2 Single Part-Throughwall Circumferential Flaw

A series of analyses for 80 and 90 percent deep, 180°, 240°, 270°, 330° and 360° long cracks was completed. Plots of the COD and average crack tip equivalent plastic strain vs. axial load for the 90 percent deep PTW cracks are shown in Figs. 4-2a-b, respectively. Except for the 360° crack, the critical values of COD 0.97 mm (0.038 in.) and plastic strain (100 percent) are predicted to be attained at about the same axial load. For the 360° crack, ligament rupture is predicted to occur by the onset of tensile cracking initiation. Similar plots for the 80 percent PTW cracks are shown in Figs. 4-3a-b, respectively. The critical COD for the 80 percent deep cracks is 0.19 mm (0.0076 in.) In most cases, the controlling criterion for ligament rupture is the critical crack tip plastic strain = 100 percent.

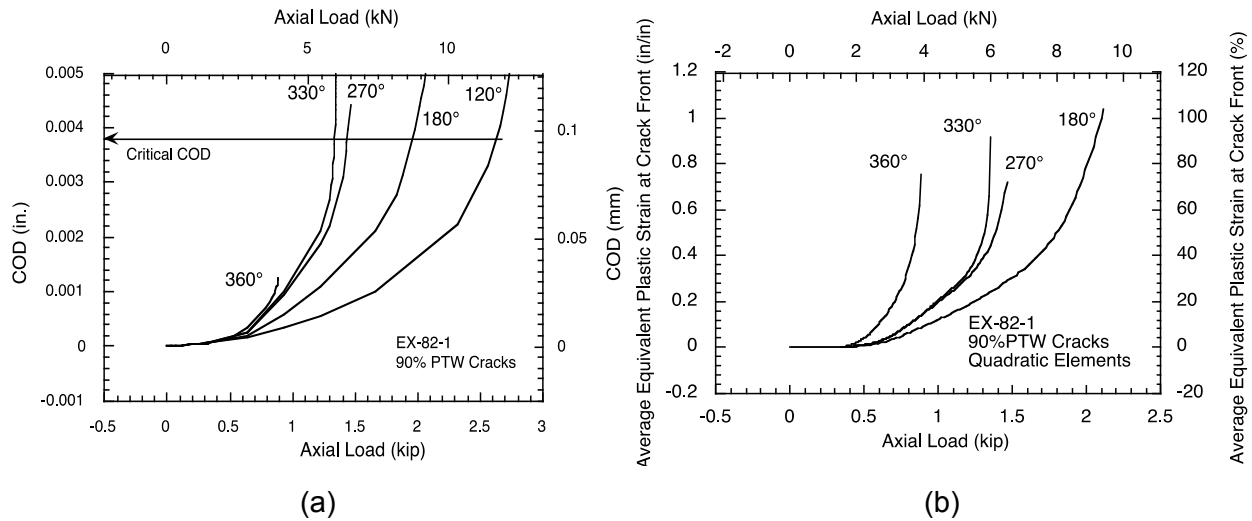


Figure 4-2 Variation of (a) COD and (b) average crack tip plastic strain with axial load for various 90 percent deep PTW cracks

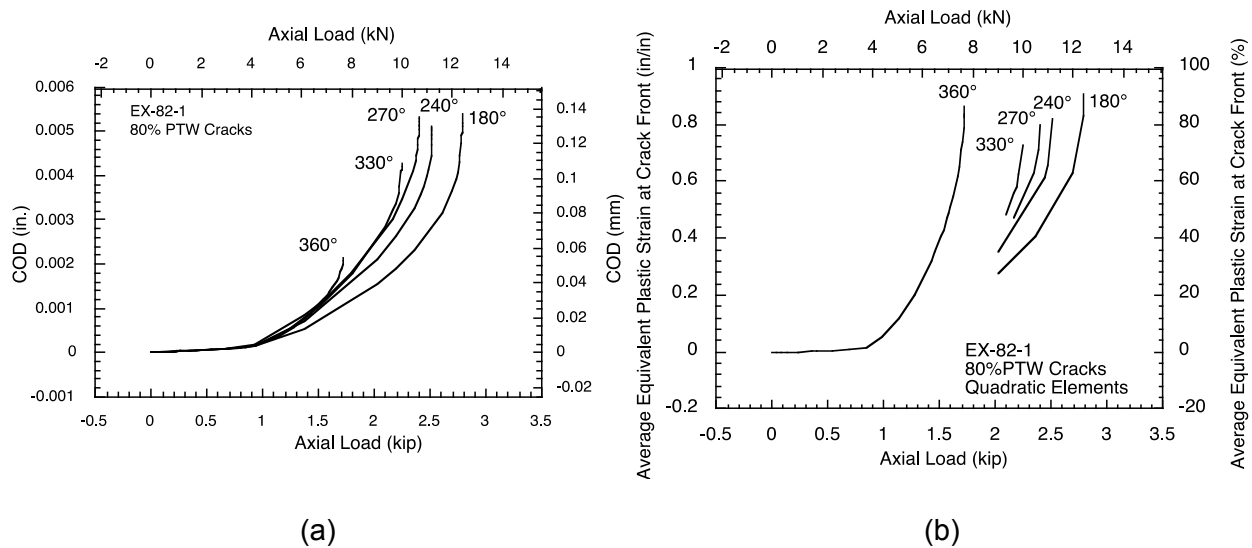


Figure 4-3 Variation of (a) COD and (b) average crack tip plastic strain with axial load for various 80 percent deep PTW cracks

The results of all the critical axial loads as functions of crack angle are plotted in Fig. 4-4. It should be noted that any PTW crack would have to experience ligament rupture prior to experiencing unstable burst. As the axial load on a crack of given length and depth is increased (i.e., load point projected vertically upwards), two different situations may arise depending on the sequence at which the projection would intersect the various depth curves. For example, the projected load line for a 180°/90 percent PTW crack intersects the 90 percent PTW curve at 50 kN (11.2 klbf) before intersecting the 100 percent TW crack at 70 kN (15.7 klbf), which would indicate that the crack would experience ligament rupture at 50 kN (11.2 klbf) before unstable burst at 70 kN (15.7 klbf). On the other hand, a similar projection for a 240°/80 percent PTW crack would intersect the 100 percent TW curve at 50 kN (11.2 klbf) before intersecting the 80 percent PTW curve at 64 kN (14.4 klbf), which would indicate that the crack would undergo ligament rupture first at 64 kN (14.4 klbf) following which it would immediately experience unstable burst because 64 kN (14.4 klbf) is > 50 kN (11.2 klbf).

As we noted earlier, the calculated axial loads during MSLB reported in the literature varied from 2891 N (650 lbf) (best estimate) to 13344 N (3000 lbf) (bounding value). Following the logic in the previous paragraph, Figure 4-4 shows that any circumferential crack <math> < 330^\circ </math>, irrespective of depth, will survive the best-estimate axial load for MSLB. Any 100 percent TW crack <math> < 170^\circ </math> will survive the bounding value of the axial load during MSLB. With slight extrapolations we can also conclude that any 90 percent PTW crack <math> < 100^\circ </math> and any 80 percent TW crack <math> < 140^\circ </math> will survive the bounding value of the axial load 13344 N (3000 lbf) during MSLB. Also, any 90 percent deep PTW crack >math> > 280^\circ </math> and any 80 percent deep PTW crack >math> > 190^\circ </math> will experience unstable rupture immediately after ligament rupture. On the other hand, any 90 percent deep PTW crack <math> < 280^\circ </math> and any 80 percent deep PTW crack <math> < 190^\circ </math> will undergo ligament rupture first and will require further increase of loading before experiencing unstable rupture.

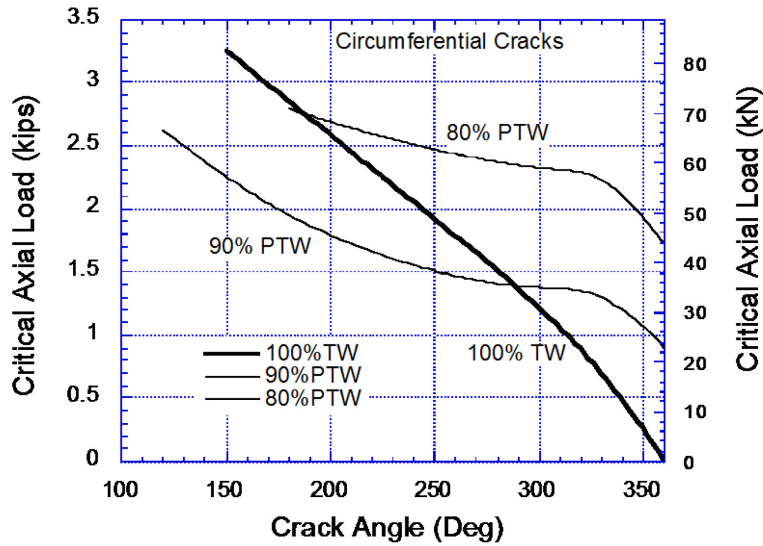


Figure 4-4 Critical axial loads for various circumferential crack lengths

5 DISCUSSIONS AND CONCLUSIONS

In general, the findings of this report suggest that cracks must be relatively severe to cause unstable tearing during accident scenarios. In accordance with Title 10 of the *Code of Federal Regulations*, Part 50, Appendix A, the General Design Criteria, Criteria 14, 15, 30, 31, and 32, the integrity of steam generator tubes must be maintained. Specifically, 10 CFR 50 Appendix A Criterion 31 states that "the reactor coolant pressure boundary shall be designed with sufficient margin to assure that when stressed under operating, maintenance, testing, and postulated accident conditions (1) the boundary behaves in a non-brittle manner and (2) the probability of rapidly propagating fracture is minimized. The design shall reflect consideration of service temperatures and other conditions of the material under operating, maintenance, testing, and postulated accident conditions and the uncertainties in determining (1) material properties, (2) the effects of irradiation on materials, (3) residual, steady state and transient stresses, and (4) size of flaws." The data developed and documented in this report serve to aid in ensuring compliance by informing staff of the expected behavior of SG cracks under accident conditions.

5.1 LOCA

The analysis documented in this NUREG/CR shows that the longest 100 percent TW single flaw that will survive LB LOCA is 110°. Thus, any 100 percent TW crack longer than 110° is predicted to fail unstably during the LB LOCA loading. For comparison, a submittal by AREVA with regard to LB LOCA analysis of Davis Besse reported that the best-estimate (50/50) limit for a 100 percent TW circumferential crack is 14 mm (0.55 in.) (i.e., 107°) (Ref. 7).

The tensile rupture initiation model predicts that any 360° crack shallower than 31 percent deep will survive the LBLOCA loading. The net section flow theory predicts the critical depth to be 38 percent. For comparison, the EPRI guideline for SG Integrity Assessment predicts the critical depth to be 42 percent (Ref. 15).

A single ≤60 percent deep, ≤135° PTW crack will not experience either ligament rupture or unstable burst during LB LOCA. A single >60 percent deep, ≤110° PTW crack may, depending on length/depth, either experience ligament rupture without unstable burst or survive LB LOCA without ligament rupture or unstable burst. A single ≥60 percent deep, ≥135° PTW crack will experience unstable burst. Industry estimated that a single 60 percent deep PTW flaw will remain stable if the circumferential extent is < 150° (Ref. 2).

3x30° (land length = 4 mm [0.16 in.]) and 3x45° (land length = 6 mm [0.24 in.]) 60 percent deep PTW wear marks are predicted to survive LB LOCA without ligament rupture or unstable burst. The longest individual length of 3x90 percent deep wear marks that will survive the LB LOCA cooldown ($\Delta T = 220^{\circ}\text{C}$ [428°F]) is 26.5°. It is predicted that both 3x30°x90 percent PTW and 3x45°x90 percent PTW cracks will remain stable after ligament rupture during LB LOCA.

In the LB LOCA analysis of Davis Besse, AREVA cites experimental data that show wear scar depth has to be >92 percent deep for it to pop through (i.e., experience ligament rupture, Ref. 7). Also, 100 percent deep wear scars can meet LB LOCA structural integrity requirement at 95/50 confidence.

In the LB LOCA analysis of TMI-1, AREVA reported that the allowable pop-through depth for a TSP wear scar is 78 percent through-wall and that the ligament pop-through will not lead to a tube "burst" (Ref. 8).

5.2 MSLB and FWLB

A review of the literature showed that the total axial tensile load on an OTSG tube during MSLB varies as a function of time as well as location with respect to the tubesheet. It increases monotonically from the center of the tubesheet towards the outermost tubes. There are two sources for the axial load –the first which is generally dominant, is due to the temperature difference between the tube and the SG shell and the second is a mechanical component created by pressure-induced tubesheet bowing. The actual magnitude of the axial loads in the tubes has a significant variation between plants. A best estimate value for the maximum axial load is 2.9 kN (650 lbf) and a bounding value is 13.3 kN (3000 lbf). There is a consensus that the stresses due to axial loads on a tube during FWLB are generally either too low or compressive and do not challenge the integrity of the tubes with circumferential cracks.

The analysis showed that single cracks $< 330^\circ$, irrespective of depth, will survive the best-estimate axial load for MSLB. Any 100 percent TW crack $< 170^\circ$ will survive the bounding value of the axial load during MSLB. 90 percent PTW cracks $< 100^\circ$ and 80 percent TW cracks $< 140^\circ$ will survive the bounding value of the axial load 13.3 kN (3000 lbf) during MSLB without ligament rupture or unstable tearing. Also, under increasing loading, 90 percent deep PTW cracks $> 280^\circ$ and 80 percent deep PTW cracks $> 190^\circ$ will experience unstable rupture immediately after ligament rupture. On the other hand, 90 percent deep PTW cracks $< 280^\circ$ and 80 percent deep PTW cracks $< 190^\circ$ will undergo ligament rupture first (i.e., will leak) and will require further increase of loading before experiencing unstable rupture.

6 REFERENCES

1. B&W Topical Report BAW- 1847, Rev. 1, "Leak-Before-Break Evaluation of Margins Against Full Break for RCS Primary Piping of B&W Designed NSS," September 1985.
2. B&W Topical Report BAW-2374, "Justification for Not Including Postulated Breaks in Large-Bore Reactor Coolant System Piping in the Licensing Basis for Existing and Replacement Once-Through Steam Generators", July, 2000.
3. B&W Topical Report BAW-10146 "Determination of Minimum Required Tube Wall Thickness for 177-FA Once-Through Steam Generators," October, 1980.
4. TMI Report ECR #02-01121, Revision 2, Inspection Acceptance Criteria and Leakage Assessment Methodology For TMI OTSG Kinetic Expansion Examinations", Oct 14, 2005.
5. Three Mile Island Nuclear Station, Unit 1 (TMI-1) Steam Generator Tube Kinetic Expansion Inspection and Repair Criteria, Nov. 8, 2006.
6. Letter from D. Baxter, Vice President Oconee Nuclear Station to U.S. NRC, dated September 16, 2009 (ML092660116).
7. Response to Specific Issues on Tube Integrity Analyses performed for the large break loss of coolant accident at the Davis –Besse Nuclear Power Station, Unit No. 1, February 10, 2010 (ML100491091).
8. "Summary Report for Qualification of Enhanced Once Through Steam Generators (EOTSGs) for LBLOCA Loading", AREVA Report 51-9125139-001, January, 2010.
9. A. A. Wells, "Unstable Crack Propagation in Metals: Cleavage and Fast Fracture," Proc. Of the Crack Propagation Symposium, Vol. 1, paper 84, Cranefield, UK, 1961.
10. F. M. Burdekin and D. E. W. Stone, "The Crack Opening Displacement Approach to Fracture Mechanics in Yielding Materials," J. of Strain Analysis, Vol. 1, 1966, pp.145-153, 1966.
11. J. R. Rice, "A Path Independent Integral and the Approximate Analysis of Strain Concentration by Notches and Cracks," J. of Applied Mechanics, Vol. 35, pp. 379-386 (1968).
12. Steam Generator Tube Integrity Program - Phase 1 Report, Prepared by J. M. Alzheimer et al., NUREG/CR-0718, Battelle Pacific Northwest Laboratory, September, 1979.
13. M. Kozluk, D.G. Martin and B.E. Mills, "Ontario Power Generation's Steam Generator Tube Testing Project," Presented at the 4th CNS International Steam Generator Conference, Toronto, Ontario, Canada, May 5-8, 2002.
14. S. Pagan and C. Regan, "Characterization and Burst Pressure Testing of Alloy 800 Steam Generator Tubing with Axial Slots," Presented at the International Steam Generator Tube Integrity Program Semi-Annual Meeting hosted by the Canadian Nuclear Safety Commission, Toronto, Canada April 16-17, 2013.
15. Steam Generator Integrity Assessment Guidelines, Revision 2, EPRI, Palo Alto, CA: 2006. 1012987.

<p>NRC FORM 335 (12-2010) NRCMD 3.7</p> <p style="text-align: center;">U.S. NUCLEAR REGULATORY COMMISSION</p> <p style="text-align: center;">BIBLIOGRAPHIC DATA SHEET <i>(See instructions on the reverse)</i></p>	<p>1. REPORT NUMBER (Assigned by NRC, Add Vol., Supp., Rev., and Addendum Numbers, if any.) NUREG/CR-7225</p>	
<p>2. TITLE AND SUBTITLE Stability of Circumferential Flaws in Once-Through Steam Generator Tubes Under Thermal Loading During LOCA, MSLB, and FWLB</p>	<p>3. DATE REPORT PUBLISHED</p>	
	<p>MONTH November</p>	<p>YEAR 2017</p>
<p>5. AUTHOR(S) Saurin Majumdar</p>	<p>4. FIN OR GRANT NUMBER Y6582</p>	
	<p>6. TYPE OF REPORT Technical</p>	
<p>8. PERFORMING ORGANIZATION - NAME AND ADDRESS (If NRC, provide Division, Office or Region, U. S. Nuclear Regulatory Commission, and mailing address; if contractor, provide name and mailing address.) Argonne National Laboratory Argonne, IL 60439</p>	<p>7. PERIOD COVERED (Inclusive Dates)</p>	
	<p>9. SPONSORING ORGANIZATION - NAME AND ADDRESS (If NRC, type "Same as above", if contractor, provide NRC Division, Office or Region, U. S. Nuclear Regulatory Commission, and mailing address.) Division of Engineering Office of Nuclear Regulatory Research U.S. Nuclear Regulatory Commission Washington, DC 20555</p>	
<p>10. SUPPLEMENTARY NOTES</p>		
<p>11. ABSTRACT (200 words or less) Axial thermal loads during loss of coolant, main steam line break and feed water line break accident conditions may cause circumferential flaws in steam generator tubes to sever in once-through steam generators (OTSGs). Finite element models were used to examine the combined effects of thermal loads, tube size, flaw size, and accident conditions that result in tube failure.</p>		
<p>12. KEY WORDS/DESCRIPTORS (List words or phrases that will assist researchers in locating the report.) PWR steam generator (SG) steam generator tube</p>	<p>13. AVAILABILITY STATEMENT unlimited</p>	
	<p>14. SECURITY CLASSIFICATION (This Page) unclassified</p>	
	<p>(This Report) unclassified</p>	
	<p>15. NUMBER OF PAGES 53</p>	
<p>16. PRICE</p>		



Federal Recycling Program



UNITED STATES
NUCLEAR REGULATORY COMMISSION
WASHINGTON, DC 20555-0001

OFFICIAL BUSINESS



NUREG/CR-7225

**Stability of Circumferential Flaws in Once-Through Steam Generator Tubar Thermal
Under Thermal Loading During LOCA, MSLB and FWLB**

November 2017